

Axial Flux Permanent Magnet Motor Csiro

New frame design, analysis, steady state model and comparison to radial flux permanent magnet motor Biel

R. Al Zaher

Master of Science Thesis

Axial Flux Permanent Magnet Motor Csiro

**New frame design, analysis, steady state model and comparison to
radial flux permanent magnet motor Biel**

MASTER OF SCIENCE THESIS

For the degree of Master of Science in Mechanical Engineering at Delft
University of Technology

R. Al Zaher

April 5, 2010

Faculty of Mechanical, Maritime and Materials Engineering (3mE) · Delft University of
Technology



The work in this thesis was supported by Nuon Solar Team 2007 and 2009. Their cooperation and support is hereby gratefully acknowledged.



Copyright © Biomechanical Engineering (BMECHE)
All rights reserved.

DELFT UNIVERSITY OF TECHNOLOGY
DEPARTMENT OF
BIOMECHANICAL ENGINEERING (BMECHE)

The undersigned hereby certify that they have read and recommend to the Faculty of
Mechanical, Maritime and Materials Engineering (3mE) for acceptance a thesis
entitled

AXIAL FLUX PERMANENT MAGNET MOTOR CSIRO

by

R. AL ZAHER

in partial fulfillment of the requirements for the degree of
MASTER OF SCIENCE MECHANICAL ENGINEERING

Dated: April 5, 2010

Supervisor(s):

Prof.dr.ir. P.Wieringa

Ir. S. de Groot

Dr.Ir. Henk. Polinder

Reader(s):

Ir. J. Spronck

Axial flux permanent magnet motor Csiro: New frame design, analysis, steady state model and comparison to radial flux permanent magnet motor Biel

Rabih Al Zaher, Mechanical Engineering Msc student, *Graduation professor: Prof. P. Wieringa, Supervisors: Ir. H. Polinder, Ir. S. de Groot*

Abstract—This paper analyses, models and presents a new frame design for the Csiro electric drive for solar cars. The main objective is to determine whether Csiro motor (CM) is more efficient than the Biel motor (BM). To do that, performance tests were conducted and compared with both drives. Results showed that the CM is more efficient at low torques. The same results were used to derive and validate a steady state model for the CM. The Model is based on four major losses in the CM. Using the model it was possible to determine the areas where improvements were possible to boost the efficiency, to optimize the mechanical design and to calculate the losses and efficiency of the CM when subjected to some certain load.

Index Terms—Axial/radial flux permanent magnet brushless DC motor, Ironless stator, efficiency, steady state modeling, drive train, in-wheel motor

I. INTRODUCTION

THE solar car Nuna has been very successful winning the World Solar Challenge (WSC) in 2001, 2003, 2005, 2007 (figure 1) and was second in 2009. The WSC is a 3023 km race through Australia. Until 2007, Nuna was driven by a drive train consisting of an in-wheel Radial flux permanent magnet motor (RFPM) motor called BM and a motor controller. It was custom developed and built for the WSC of 1993 at the Fachhochschule of Biel for their solar car Spirit of Biel II. It was one of the first in-wheel motors used in WSC in 1993. The Biel drive train (BDT) was analyzed and tested in 2005 by G. Arkestein and E. De Jong [1]. They performed a wide range of tests in order to quantify and model the efficiency and losses of this drive train at several voltages, speeds and torques. However, all direct competitors of Nuna use an in-wheel Axial flux permanent magnet motor (AFPM) motor, called Csiro. This motor was especially developed in 1996 for the WSC.



Fig. 1. Photograph of Nuna4 during World solar challenge in 2007.

A. Description of axial flux and radial flux permanent magnet motor

In a RFPM motor, armature windings and magnets are arranged in a radial way. These magnets are placed parallel to the shaft of the machine. In an AFPM machine, armature windings and magnets are arranged axially. The magnets are perpendicular to the shaft direction whereas the flux lines are parallel to it. Figure 2 shows schematic figure an AFPM and RFPM motors.

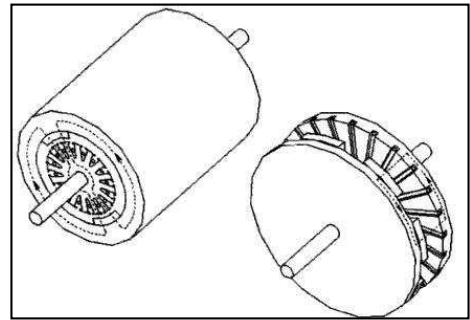


Fig. 2. Flux lines in radial (left) and axial (right) motors

B. Csiro motor

The Csiro electric motor for solar cars is an ironless brushless axial flux permanent magnet motor. It was developed in 1996 [4] and used with the Aurora solar Team who won with it the race in 1999. CM is available with two different magnet rings: one with surface Permanent magnets (PM) glued to steel discs and one with PMs arranged in a halfbach array. A halfbach array consists of specially arranged PM in a way that the magnetic field is increased on side and reduced to nearly zero on the other side. No backing steel is used in such an array. This increase in the magnetic field leads to motors with higher efficiencies. The efficiency of a CM with surface PM is 97.5% [4] whereas the efficiency with a halfbach array is 98.2% respectively [6]. The CM investigated in this paper is the one with surface PMs. Its specifications according to the manufacturer are shown in table I. It is delivered as a kit consisting of two rotors containing surface mounted rare earth magnets (NdFeB), a wound stator embedded in epoxy, a

position sensor and three inductors as shown in figure 3. The purchaser can then integrate the kit into a frame of directly into an inwheel frame.

TABLE I
CSIRO MOTOR SPECIFICATIONS.

Nominal speed (rad/s) ²	111
Nominal torque (Nm) ³	16.2
Efficiency (%)	97.4
Maximum speed (rad/s)	300
Maximum torque (Nm)	50.2
Approximate weight of frameless motor (kg)	10.9

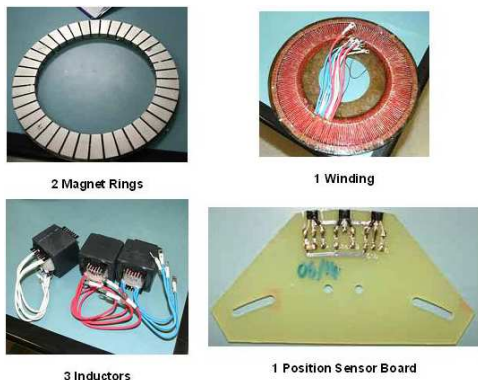


Fig. 3. Csiro motor kit components.

C. Importance of this study

Nuna won the race in Australia 4 times with BM. The specifications of CM shows however, that it is currently the most efficient motor for a solar car commercially available. A comparison study between BM and CM has not been performed. It is an interesting comparison because those motors differ in type: BM is a RFPM motor while CM is an AFPM one with an ironless stator. Several studies showed that AFPM motors [3], [8], [9], [10], [11], [12] and [13] can be a better replacement for the more conventional RFPM motors due to the fact that AFPM have higher torque to volume/mass ratio's. Furthermore, Csiro claim that the efficiency at nominal torque and speed is 97.5%. This is questionable because this value is based on a simplified analytical model where the influence of the mechanical design is neglected [4]. For example, bearing losses are dependent on the bearing choice and windage losses are caused by the frame design. Moreover, there hasn't been any published testing results confirming the claim of Csiro. Therefore, a performance test is needed in order to quantify the efficiency of CM.

This paper presents in the first section a new mechanical design for the CM. The proposed design differs radically from previous designs which are mostly based on the Aurora design [4]. The advantages of this design for a solar car are then discussed. The second section presents the efficiency tests performed on a specially designed test setup at different torques and speeds. The results are then compared with Biel motor efficiencies [7] and clarified. The third section, a steady state model based on major losses in the motor is derived in

order to predict its efficiency at a given speed and torque. Finally, the final optimized mechanical design is presented.

II. MECHANICAL DESIGN

Because the Csiro electric motor is delivered as a kit, a mechanical housing is needed in order to turn it into an in-wheel motor. The mechanical design of an electric motor has direct consequences on the performance of the motor, for example bearing and windage losses are caused by the motor frame and should be kept as low as possible. The most important requirements are minimum weight, compactness, reliability and ease of maintenance.

A. Design description

The in-wheel motor mechanical design which is shown on the left in figure 5 consists of four main components: rotor frame for the first magnet ring fixation with a 16 inch rim for tire mounting, rotor cover for the second magnet ring fixation, a shaft/hub combination for the support of the stator and position sensor and finally a double groove ball bearing. Finite element analysis is conducted to optimize the design.

B. Comparison to conventional design and advantages of the new design

A conventional housing design is shown on the right in figure 5. During the assembly of the conventional design special care should be given not to damage the bearing; the magnetic attraction force can cause misalignments between shaft, motor frame and bearing. Bearing damage can occur. This problem is more severe when dismantling the motor. The new suggested frame is designed in such a way that this problem can never occur: there is no contact between motor cover and bearing. The magnetic attractive force between the magnet rings does not act in anyway on the bearing. In the conventional design, this magnetic force is acting on both sides of the motor frame in which a bearing is mounted. The bearing can be damaged during assembly, dismantling or service. Moreover, the weight is greatly reduced due to the fact that the motor cover has a donut shape with an inner diameter slightly smaller than the magnet ring left in figure 5. Further, the width of the motor is just 60mm and compared to the conventional design is much smaller figure 4. It is even smaller than the Michelin radial tire which is 65mm as shown on the right of figure 4.

III. PERFORMANCE TEST

Csiro Research group claims [4] that the efficiency of CM is 97.5% at nominal speed and torque with an airgap of 1.75mm. With a new custom made motor frame the steady-state performance is tested in order to quantify the efficiency of the motor. The mechanical design has direct influence on the efficiency of the motor: losses are caused by both the friction in the bearing and the aerodynamic drag of the rotating frame.

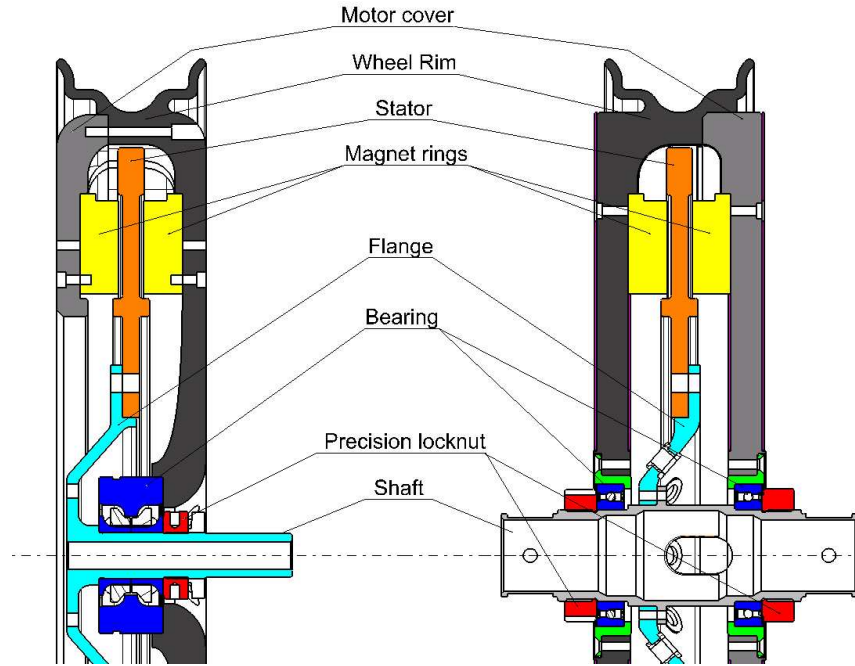


Fig. 5. Left: Motor, Csiro motor with new mechanical design investigated in this paper, right: Test load, Csiro motor based on the Aurora solar team motor design [4] and [5]



Fig. 4. Photograph of Csiro inwheel motor assembled prototype.

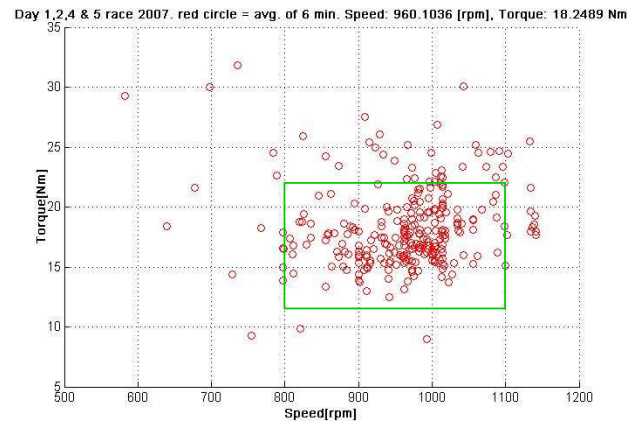


Fig. 6. Average speed and torque of World Solar Challenge (WSC) in 2007.

A. Defining the operating conditions

During the race in Australia, Nuna drives mostly at a constant speed that is dictated by a cruise control system. Depending on several factors such as battery state of charge, road conditions, torque requirements, weather conditions such as sun intensity, cross wind speeds, clouds density etc., Nuna developed a strategy program to calculate the optimal speed. From telemetry data of the race in 2007, the average speed and torque were 960.1 rpm and 18.25 Nm. Figure 6 shows the speeds and torques Nuna4 drove during the race. Each red dot is an average of speed and torque of 6 min. Therefore, based on those results, efficiency tests were conducted for the speeds of 800, 900, 1000, 1100rpm with torque values varying between 10 and 22 Nm.

B. Test setup description

In order to conduct the tests, a special test setup was designed in which two solar car in-wheel motors (CM and/or BM) can be mounted as shown in figure 7. In order to remove any possible mechanical losses due to misalignments between the motors shafts, the mounting frame is designed in such a way that the mounted motors are perfectly aligned. During testing, one motor acts as a motor the other one acts as a load (generator). The load is defined by a variable resistance. Between the two motors a torque sensor is placed in order to measure the torque delivered by the tested motor. For the test, two CMs are used with different mechanical housing designs. One motor is fitted with the new mechanical design and the other one is fitted with the conventional design see figure 5. Further, a power analyzer is used to measure the power going

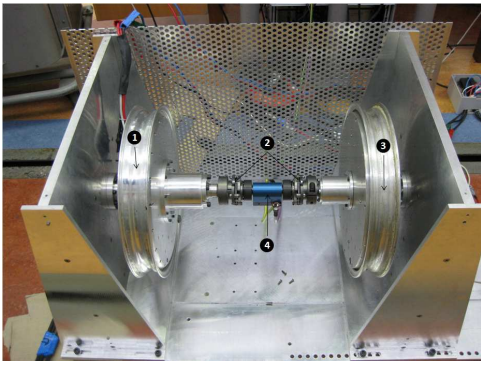


Fig. 7. Test frame for mounting the motors: (1) new motor frame design, (2)couplings, (3)standard AFPM motor frame design , (4)torque sensor.

into the motor controller and the one to the motor. Being recommended by Csiro, two Tritium WaveSculptor inverters are used to control the motors. The whole test setup is shown in figure 8.

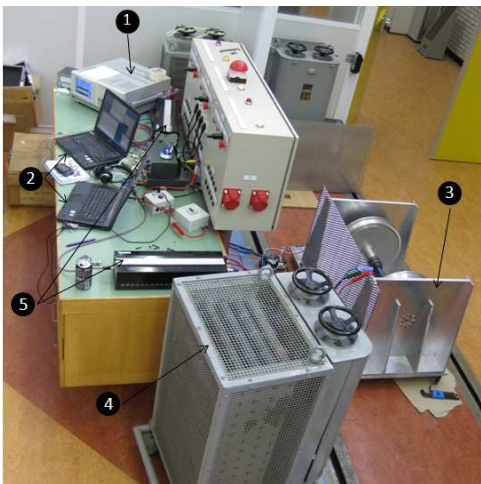


Fig. 8. Laboratory set for measuring the driver performance at steady state:(1) power analyzer, (2) two laptops for communication with the motor controllers and torque sensor and logging measured data,(3) test frame for mounting the motors,(4) variable resistance,(5) Tritium motor controllers.

C. Test procedure

As mentioned earlier, tests were conducted for the speeds of 800, 900, 1000 and 1100 rpm with torque varying between 10 and 22 Nm. In this torque range up to 17 set points were tested. Each set point was tested for four minutes for mainly two reasons. The first is to have enough points to calculate the torque mean. The second is practical to have enough time to write the power measurements of the power analyzer in the excel sheet. The torque sensor frequency was set to 100Hz while the power analyzer was sampled at a frequency of 5MHz. Tests were performed twice with a week time between the first tests and the second tests. Moreover, the second test results showed little difference with the first test results. Temperature in the laboratory varied slightly during testing between 20.5 and 23 degrees Celsius.

D. Results

The test results are shown here below. In each graph several lines are plotted: motor controller efficiency (up-red), motor efficiency (middle-purple) and the total set efficiency (bottom-blue). The curves are the average of two performed tests. The results of each test are given for each efficiency by a dot and a cross. The difference between the two tests is very small and does not exceed 0.3%.

E. Efficiency comparison Csiro motor (CM) with Biel motor (BM)

The efficiency plot in figure 10 shows that CM is more efficient up to a certain torque. In the 3D plot, the efficiency surface plot of each motor is given. The CM efficiency surface intersect with the BM efficiency surface plot at a torque varying from 19 to 22Nm for speeds varying from 800 to 1100 rpm. In the tested range CM is up to 4% more efficient at low torque (10Nm). These results can be explained by a crucial difference between CM and BM. BM stator contains iron laminations which cause eddy currents losses that are not present in the ironless CM stator. At larger torques however, due to the absence of iron in the stator of CM large currents are needed in order to achieve the torque requirement. This will cause an increase in the copper losses. For the same high torque load, the presence of iron helps BM to use less current than CM and therefore copper loss will also be smaller. In this case the copper loss in CM is larger than both eddy currents and copper loss in BM.

IV. STEADY STATE MODELING

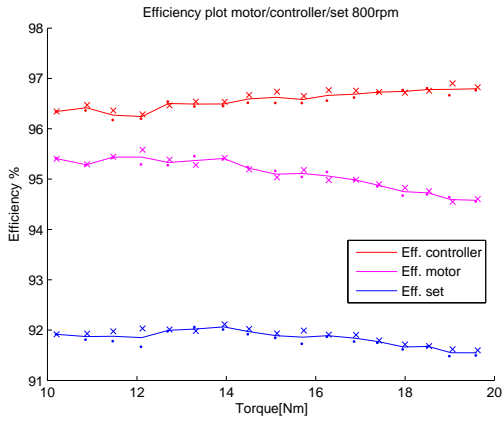
During a solar race, Nuna drives on a specially developed cruise control system. The cruising speed is mostly constant and varies gradually during the day. The genetic algorithm based software of the cruise control system uses several parameters to calculate an optimal speed. Among those parameters are weather conditions and weather forecast such as sun intensity, cross winds, humidity level and clouds density, battery state of charge at the of a racing day and the race, rolling resistance, road conditions, aerodynamics of the car and efficiency of the electric drive. The motor power consumption and efficiency is therefore needed in order to help the strategy program calculate the optimal speed at a defined speed and torque.

The steady state model is also a powerful tool to define and understand of the source of the losses in the motor. It is also used not only for strategy purposes but also to improve the motor frame design.

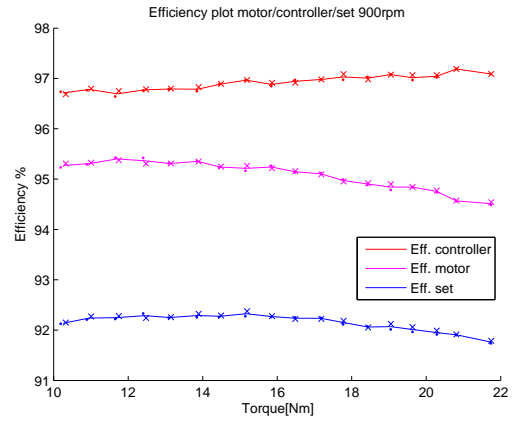
A. Assumptions

In order to derive the model some assumptions were made. The most important ones are given here below.

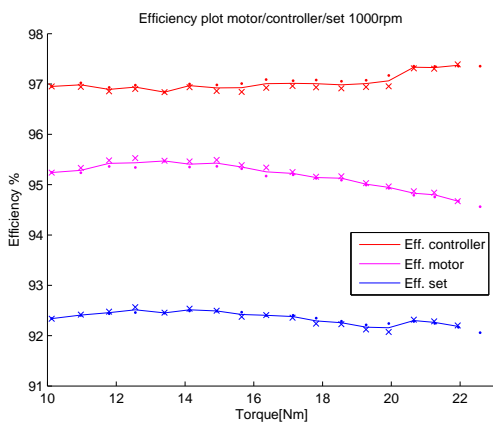
- The current is assumed to be sinusoidal
- The torque constant of the motor K_t is considered to be constant



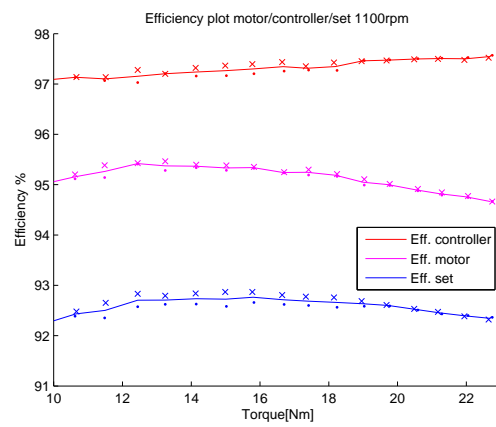
(a) 800rpm



(b) 900rpm

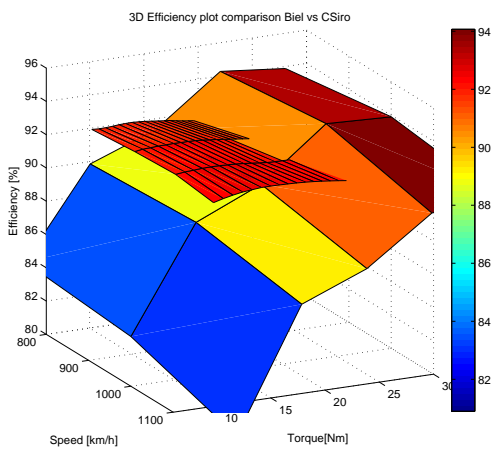


(c) 1000rpm

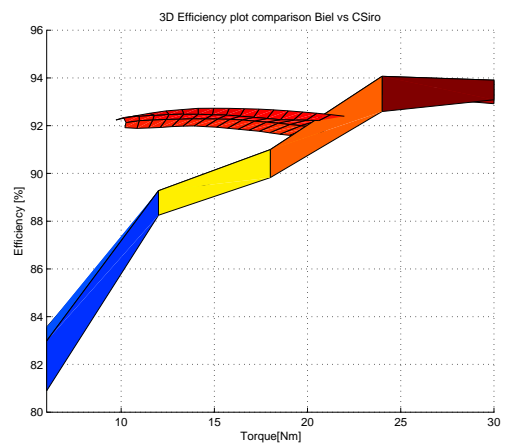


(d) 1100rpm

Fig. 9. Test results.



(a) 3D surface plot efficiencies



(b) 2D view

Fig. 10. Comparison plot Csiro motor (CM) vs Biel motor (BM).

- The influence of the temperature is not taken into consideration in the model because the temperature is relatively low (41° at 22.8Nm and 1100rpm) at steady state conditions at low torques.

B. Equivalent circuit

In order to model the steady state performance of the Csiro the equivalent circuit is needed [2]. The equivalent circuit of the CM drive is presented in figure 11, where R and X_w are the winding resistance and leakage reactance resp., E is the EMF induced in the stator winding, X external inductors, U_{dc} terminal voltage, i is the rms value of the current.

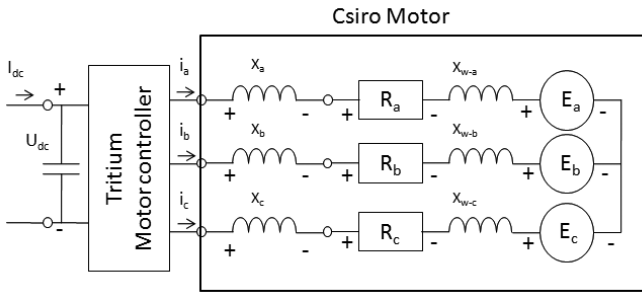


Fig. 11. Csiro drive equivalent circuit.

C. Losses and efficiency definition

The losses in the motor can be both electrical and mechanical. Only major losses of both electrical and mechanical aspects are taken into consideration in the derivation of the steady state model. The electrical losses are conductor losses (copper losses, eddy current losses of the copper windings and inductor losses). The mechanical losses also known as rotational losses are known as Bearing losses (BL) and Windage losses (WL). The total loss of the motor is equal to the sum of the mentioned losses.

$$P_{loss} = P_{elec} + P_{rot} = P_c + P_e + P_{ind} + P_b + P_{wind} \quad (1)$$

where:

P_c = conductor losses [W]

P_e = eddy current losses [W]

P_{rot} = rotational losses [W]

P_{ind} = inductor losses [W]

P_b = bearing losses [W]

P_{wind} = windage losses [W]

The mechanical power output of the motor:

$$P_{out} = \tau \cdot \omega_m \quad (2)$$

where:

τ = motor delivered torque [Nm]

ω_m = motor rotational speed [rad/s]

The efficiency of the motor is calculated as follows [2] and [6]:

$$\eta_{motor} = \frac{P_{out}}{P_{out} + P_{loss}} \quad (3)$$

Copper losses (CL) are calculated as follows:

$$P_c = 3Ri^2 \quad (4)$$

It is temperature dependent as the resistance increase with increasing temperature

$$R = R_0(1 + 0.0039(T_w - T_0)) \quad (5)$$

Where:

R_0 = Winding resistance at 20°[Ohm]

$T_0 = 293[K]$ Winding Temperature at 20°

i = RMS current value per phase [A]

T_w = Winding temperature [K]

The influence of the temperature change is so small that it is kept out of consideration in the model derivation.

Eddy current losses:

Eddy current losses in the stator windings can be both analytically calculated or experimentally tested. In order to analytically determine them, some parameters should be known such as the radius R of the winding conductor, resistivity ρ and length l of the conductors. However, the information needed is not available. Therefore eddy current losses are determined experimentally.

The motor is driven at no load at several speed. The mechanical power needed to drive the motor is measured. This power is equal to the sum of eddy current losses and rotational losses. The same experiments are then repeated with a dummy stator. The mechanical power difference between the first and second tests is equal to the eddy current losses. Csiro specifies eddy current losses to be equal to 2.1W at nominal speed. However measurements showed the eddy current losses to be much higher. In table II eddy current losses are given for the speeds 800, 900, 1000 and 1100 rpm.

Rotational losses: The rotational losses consists of two components: BL and WL. BL are linear with the speed whereas the WL have a cubic relation with the rotational speed.

$$P_{rot} = P_b + P_{wind}[W] \quad (6)$$

$$P_b = 0.06K_{fb}(m_r + m_{sh})\omega_m[W] \quad (7)$$

Where:

$m_r = 15.2$, rotor mass: consisting of motor frame and two magnet rings [kg]

$m_{sh} = 1.5$, shaft mass: consisting of the shaft and stator [kg]

$K_{fb} = 1$, bearing friction coefficient: the coefficient taken to be equal to one as the bearing is light tensioned added to the fact that the motor is hanging in the test setup and not in the car.

$$P_{wind} = \frac{1}{2}c_f\rho(2\pi\omega_n)^3(R_{out}^5 - R_{sh}^5)[W] \quad (8)$$

Where:

$Re = \rho \frac{R_{out} v}{\mu}$ Reynolds number ρ is the specific density of air $v = 2\pi R_{out} \omega$ is the linear velocity at the outer radius R_{out} μ is the dynamic viscosity of the air $c_f = \frac{3.87}{\sqrt{Re}}$ Drag coefficient

Inductor losses: The induction losses includes two components: copper losses and yoke losses as defined in [6]. Those are defined as:

$$P_{ci} = R_{ci} i^2 \quad (9)$$

$$P_{yi} = 2.7 \cdot 10^{-6} i^3 f \quad (10)$$

Where: f = fundamental frequency of excitation [6]

D. Model results

The model results are shown in figure 12 together with the data plot of the motor efficiency. The difference between measured and modeled steady state performance is very small.

V. FINAL FRAME DESIGN

After having extensively tested the prototype of the new mechanical design of the motor, some modifications were needed in order to increase the efficiency of the Csiro drive as much as possible. In order to prove the benefits of some of the modifications extra tests were conducted. Since little modifications can be made on the electrical part of the motor most suggestions are mechanical. in the following two paragraphs, the optimization suggestions are discussed and the final design is presented.

A. Motor optimization

It was obvious after having tested tested the Csiro motor and made the steady state model that are a lot of possibilities of improvement especially in the frame design. Most of the improvements here below were taken into the final desgin.

- **Weight reduction:**
Use of light weight materials, for example magnesium for the rotor parts and carbon for tire rim, in order to reduce the total weight of the motor and as a result reduce the bearing losses and unsprung mass. This is however limited by the load cases (magnetic attraction force between the magnet rings) and was carefully engineered with FEM programs. This will however increase the mechanical design costs.
- **Airgap width reduction:**
This increases the magnetic field density and a result less current is needed at higher torques. However, this reduces the top speed of the motor and put the mechanical design under higher stresses. Yet the increase in efficiency is quite large up to nearly 0.8% at speed of 1000rpm and 1100 rpm as shown in figure 14. It has however small influence on the windage loss as the roll test shows in figure 13.

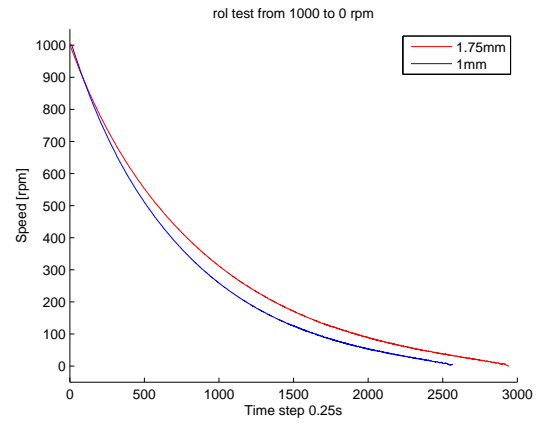


Fig. 13. Comparison roll test between 1 and 1.75 mm airgap.

- **Aerodynamics improvement:**
Smoothing the inner and the outer surfaces of the motor to reduce the windage losses. The motor was covered in foil in order to cover surface irregularities caused by bolts, inner spokes and the tire. To find out the influence of such an action, the mechanical power difference is measured between normal and foil-covered motor at no load at several speeds. The results are shown in table II.
- **Hybrid bearing:**
Using hybrid spindle bearings with 15° angular contact and ceramic balls will minimize the bearing losses. This type of bearing is the most efficient groove ball bearing available.
- **Cooling:**
Use of cooling for example during race qualification laps can be very beneficial because the motor is delivering constantly high torques during heavy acceleration and braking. The temperature of the motor will rise extremely to hit the motor thermal limit. Luckily, cooling can be easily integrated in the proposed design just by adding an adding a filter cover to the open side of the motor . Moreover, during testing a 10 degrees Celsius difference was measured between the new (open) and the conventional (closed) design.
- **Better inductors:**
Use inductors with smaller induction losses. The inductors delivered with the motor are quite over engineered. A custom made inductors with suitable induction values for CM will reduce the inductor losses. However attempts to test self-made inductors with smaller induction value failed in giving results because wrong parameters were used. Most top solar car racing teams use custom made inductors for CM.

VI. FINAL FRAME DESIGN FOR THE WSC IN OKTOBER 2009

The final design of the motor is given here below. The test results, the experience gained by building 2 concepts and the suggestions listed earlier were all taken into consideration in the the definitive design. As schematic cross section in show in figure VI. The suggestions listed above were taken into

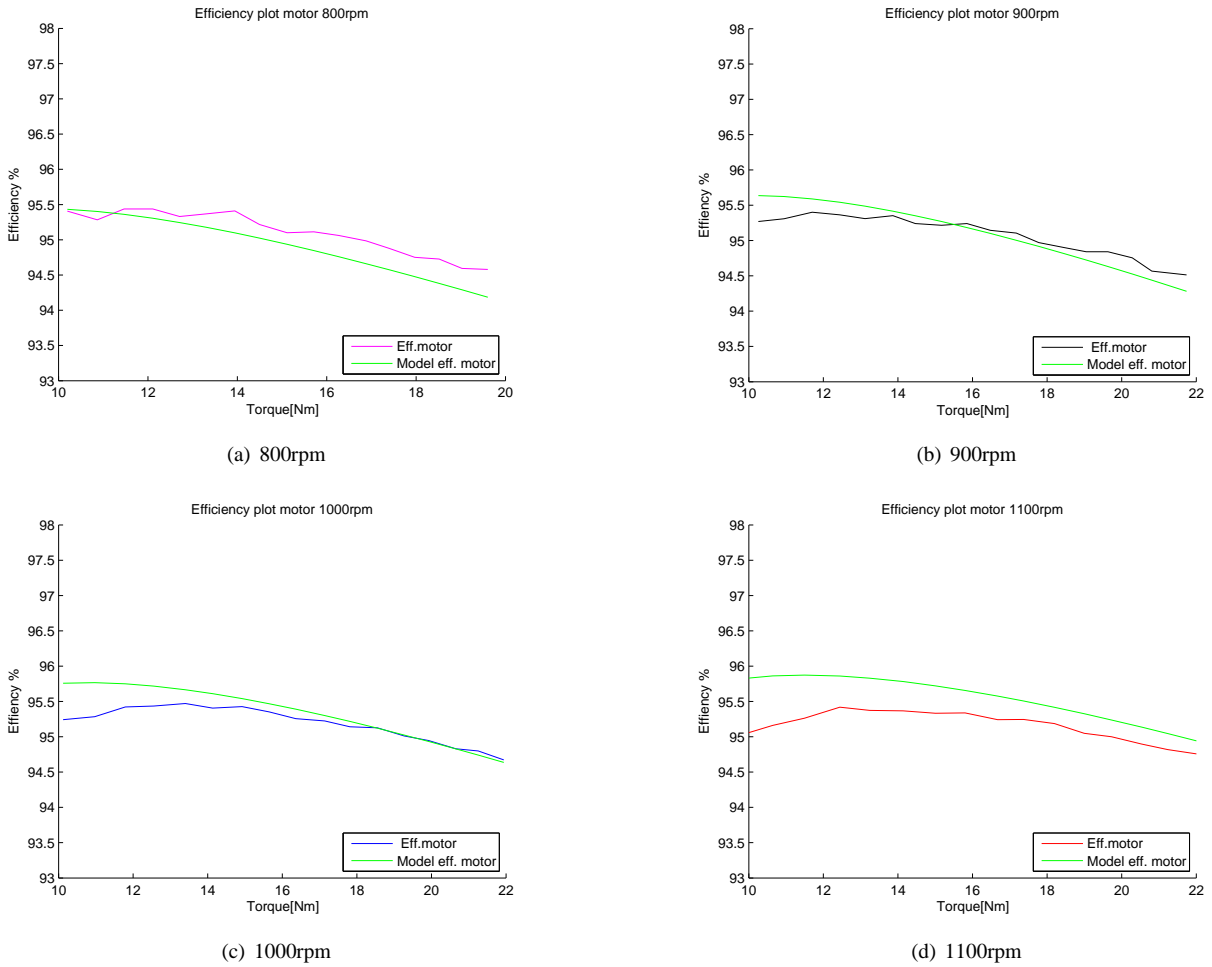


Fig. 12. Model results plots for the Csiro motor (CM) in the same speed and torque range of the performance tests.

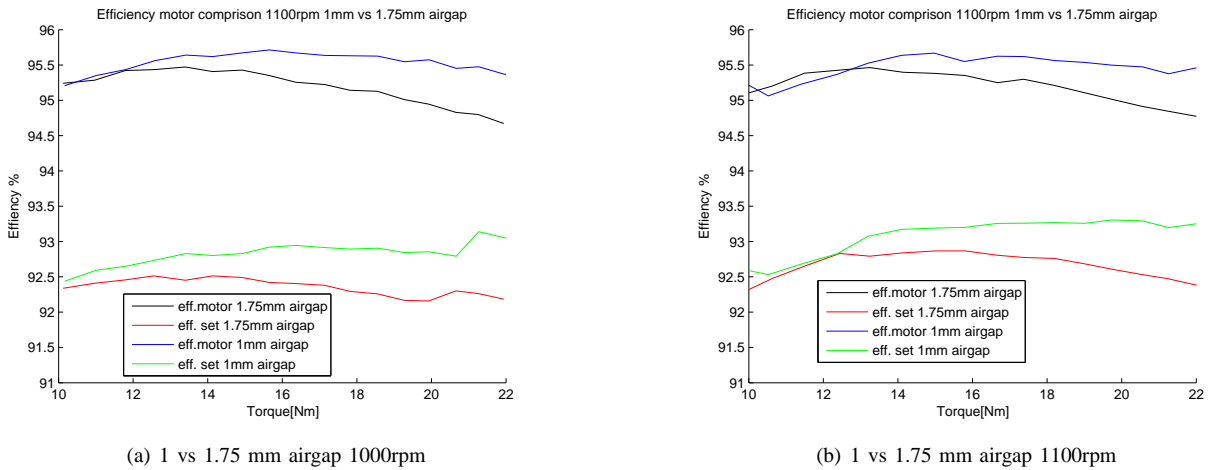


Fig. 14. Influence of airgap on motor and motor set efficiency.

TABLE II
EDDY CURRENT LOSSES AND AERODYNAMIC IMPROVEMENT.

speed [rpm]	motor with real stator[W]	with dummy stator[W]	improved aero[w]	Eddy currents losses[W]
800	16.74	12.45	12.04	4.7
900	20.71	15.31	15.08	5.6
1000	25.52	19.39	18.67	6.9
1100	30.80	24.34	22.85	7.9

consideration in the final design like for example exotic light weight materials for weight reduction: the rotor parts are made from magnesium reinforced with carbon, the shaft and all bolts are from titanium, tire rim is from magnesium, the rest of the parts is from aluminum. Another example is the use of highly efficient hybrid spindle bearing.

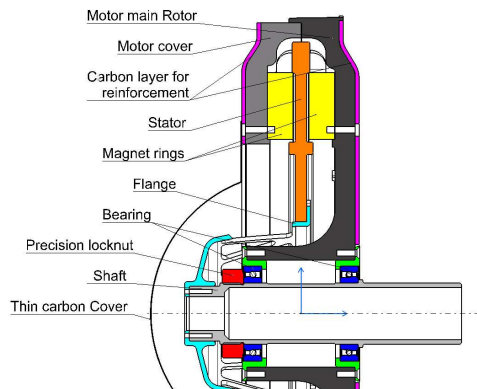


Fig. 15. Cross section of the Csiro motor with which Nuna5 drove the WSC of 2009

VII. CONCLUSIONS

This paper presented a new frame design concept for AFPM Csiro motor for solar car racing. The new design has several advantages in comparison to conventional designs: ease of assemble, dismantle and repair. Moreover, it is advantageous when it comes to weight and compactness. Test were conducted in order to confirm manufacturer specifications. Measured motor efficiency was 95.7% at a speed of 1060rpm and a torque of 16.06 Nm but with 1mm airgap. This is 1.7% less than Csiro specified at a 16.2 torque and 1060rpm speed. The results from the tests proved that in the area of interest where solar cars operates during the race, CM is more efficient than BM, due mainly to the absence of iron laminations in the stator. A model was made based on four loss sources in the motor: copper loss, eddy current loss, inductor losses and mechanical losses. Finally, a optimised motor frame was developed based on this study and used successfully in the WSC in 2009.

APPENDIX I ACRONYMS

WSC	World Solar Challenge
BDT	Biel drive train
CDT	Csiro drive train
PM	Permanent magnets
CM	Csiro motor
BM	Biel motor
AFPM	Axial flux permanent magnet motor
RFPM	Radial flux permanent magnet motor
FEM	Finite element analysis
CL	Copper losses
ECL	Eddy current losses
BL	Bearing losses
WL	Windage losses

ACKNOWLEDGMENT

The authors would like to thank Ir. P. Campagne (E2M Technologies) for his support in the design of the mechanical housing, Paul M.C. Beckers (Nuna4 Team) and Martin Deuring (Nuna5 Team) for their support in the electrical assembly and troubleshooting of the test setup.

REFERENCES

- [1] G. C. M. Arkesteijn, E. C. W. de Jong, **Loss modeling and analysis of the Nuna Solar car drive System**, *International Conference on Ecologic Vehicles & Renewable Energies*, Monaco, 2007.
- [2] Jacek F. Gieras, Rong-Jie Wang and Maarten J. Kamper, **Axial Flux Permanent Magnet Brushless Machines**, *Kluwer Academic Publishers*, The Netherlands, 2004.
- [3] Jacek F. Gieras, Mitchell Wing, **Permanent Magnet Technologies Revisited**, Marcel Dekker, inc., New York, USA 2002
- [4] B. C. Mecrow, H. C. Lovatt and V. S. Ramsden, **Design of an in-wheel motor for a solar-powered electric vehicle**. *IEE Proceeding, Electric Power Applications* 145 5 (1998), pp. 402408
- [5] Csiro electro motor Frame design CD, Aurora Solar Team
- [6] Csiro, **CSIRO Solar Car Surface Magnet Motor Kit**, <http://www.csiro.au/resources/pf11g.html>
- [7] E. C. W. de Jong, **Nuna III Power Drive Investigation**, June 2005.
- [8] M. Aydin, S. Huang and T. A. Lipo, **A new axial flux surface mounted permanent magnet machine capable of field control** *IEEE Industry Applications Society Annual Meeting*, 2002, pp. 1250-1257.
- [9] A. Parviainen, **DESIGN OF AXIAL-FLUX PERMANENT-MAGNET LOW-SPEED MACHINES AND PERFORMANCE COMPARISON BETWEEN RADIAL-FLUX AND AXIAL-FLUX MACHINES**, Lappeenranta University of Technology, Lappeenranta, Finland, April 2005.
- [10] Cavagnino, A., Lazzari, M., Profumo, F., Tenconi, A., 2001. **A Comparison Between the Axialflux and the Radial-flux Structures for PM Synchronous Motors**. In *Proceedings of IEEE Industry Applications Conference*, 36th IAS Annual Meeting, pp. 1611-1618.
- [11] Akatsu, K., Wakui, S., 2004. **A Comparison between Axial and Radial-flux PM Motor by Optimum Design Method from the Required Output NT Characteristics**. In *Proceedings of International Conference on Electrical Machines ICEM04*, Cracow, Poland, 5-8 September 2004, on CD-ROM.
- [12] Kartik Sitapati and R. Krishnan, Fellow, IEEE, **Performance Comparisons of Radial and Axial Field, Permanent-Magnet, Brushless Machines**, *IEEE TRANSACTIONS ON INDUSTRY APPLICATIONS*, VOL. 37, NO. 5, SEPTEMBER/OCTOBER 2001
- [13] N. B. Simsir and H. B. Ertan, **A comparison of torque capabilities of axial flux and radial flux type brushless DC (BLDC) drives for wide speed range applications** in *Proc. IEEE PEDS99*, vol. 2, 1999, pp. 719724.

Contents

A Mechanical design	iii
A.1 Introduction	iii
A.2 List of requirements	iii
A.3 Proposed motor frames	v
A.3.1 Description of the designs	vi
A.3.2 FEM analysis	vii
A.4 Comparison between Nuna and Aurora designs	viii
A.4.1 Advantages of the Nuna design	viii
A.4.2 Comparison test	xi
A.5 Conclusion	xiii
B Test Setup measurements	xv
B.1 Test setup	xv
B.2 Test condition and procedures	xvii
B.3 Results	xix
C Model evaluation	xxiii
C.1 Introduction	xxiii
C.2 Influence of each loss	xxiii
C.3 Conclusion	xxiv
D Matlab files	xxvii
D.1 MATLABAnalyzing torque data and computing efficiencies	xxvii
D.2 MATLABPlotting the results of all speeds and torques	xxx
D.3 MATLABModel and plot with measured data	xxxi
D.4 MATLABComparison between csiro motor and surface draw	xxxv

Appendix A

Mechanical design

A.1 Introduction

An important part of an in-wheel motor is the frame in which stator and rotor are mounted. This is even more crucial in the case of an AFPM motor. The frame of an AFPM motor is actually very challenging not only in design but also in assembly and maintenance due to the high attraction forces between the magnet rings. The Csiro electric motor is delivered by the manufacturer as a kit: 2 rings with PMs glued on steel discs, stator which consists of windings embedded in epoxy, 3 inductors and a position sensor. An important missing part of the motor is then the mechanical frame. The motor frame should be designed by the buyer and has to fulfill a set of requirements which are discussed here below.

In this appendix, a new frame design is presented and compared to the conventional design. In the first section, the requirements for the frame design to fit in a solar car are given. In the second section, two design are described and compared. For both designs FEM analysis is made presented and discussed. Finally, in the last section a choice is made for the frame design which will be used in the tests

A.2 List of requirements

The design has to comply with a long list of requirements. The most important are listed here below.

- Fit in a 16" tire: Solar cars use special tires. In order to reduce the rolling resistance, special tires were developed for solar car racing. The best available tire is the Michelin Solar Radial which is a 16inch tire. Although very expensive (250 euro), the Solar Radial is the tire with the lowest rolling resistance ever measured. Moreover, it is practically impossible to fit the CM in a tire smaller than 15 inch due to the large diameter of the stator. Another frequently used tire is the Dunlop Solar max is also 16inch.

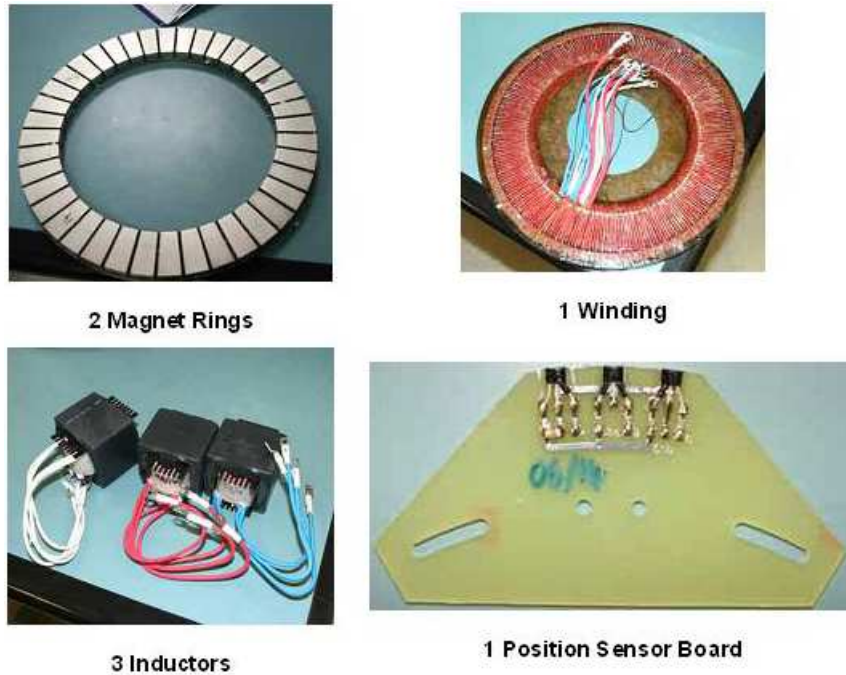


Figure A.1: Csiro electric motor components as delivered by the manufacturer

- Withstand a set of load conditions: the motor housing is subject to static and dynamical forces and must be able to withstand those forces without any failure. Those forces are:
 - **Static forces:** the strong magnetic attraction force between the rotor discs and the maximum generated torque. The magnetic force is a function of the airgap. Airgap is the distance between the magnet ring and stator. The motor frame should be able to withstand the magnetic force of 4.9kN and the maximum torque of 50.2 Nm at an airgap of 1.75mm [6]. A safety factor of 1.5 is also used to optimize the mechanical design stiffness. Moreover, the possibility of reducing the airgap is also taken into consideration and is covered by the safety factor. It is important to mention, the purpose to measure the efficiency of the motor at an airgap of 1.75mm in order to compare it to the efficiency given van Csiro.
 - **Dynamical forces:** are caused by the operational condition of the machine. The housing should be able to withstand braking with an deceleration of 1G, cornering with an acceleration of 1G and bump load caused by an obstacle of 60mm height causing an acceleration of 4G. The largest load is the 4G bump load combined with a cornering manoeuvre. The components of this load are: 4350N backward, 1100N lateral, 4825N upward.
 - **Vibrations:** Beside the forces acting on the housing, the eigen-frequencies of the housing must be higher than the operating frequencies. A modal analysis is needed to compute the eigen-frequencies and keep them above operating condi-

tions.

- **Lightweight design:** this is important for several reasons. First of all to keep the bearing losses as low as possible because the weight of the motor influences the bearing losses as discussed in paper. Second, the motor is an unsprung mass. Unsprung mass must be kept very low because it negatively influences the riding comfort of the vehicle. Finally, to keep the total weight of the car low and as a result the rolling resistance. In Nuna4 the drive train was 9.5% of the total weight of the car.
- **Compactness:** the length of the motor shaft influences the width of the rear fairing of the solar car. A smaller fairing means lower aerodynamic resistance: therefore the length of the shaft must be kept as low as possible.
- **Easy to assemble and dismantle for maintenance:** during the race a flat tire can occur or a bearing can break; therefore, the mechanical housing should allow quick and easy maintenance on the road with as much little equipment as possible. A motor change during the race is prohibited.
- **If possible adjustable airgap (AG):** smaller AG will increase the magnetic flux density in the motor. The torque is calculated following $T = K_t \cdot i$ or $T = F \cdot R$;

Where:

K_t is torque constant [Nm/A]

i is line current [A]

F is the Lorentz force caused by the interaction between the stator windings and the PM's [N]

R is the radius where resulting F is created [m]

K_t is a function of the magnetic flux density B and F is a function of both B and current i . For some torque T , when AG decreases B increases. As a result a smaller i is needed to maintain the same T . The conductor losses (Ri^2) which are a function of i , will be smaller. The efficiency of the motor will then be higher.

A.3 Proposed motor frames

Before the designs are discussed, an important issue in designing AFPM motor frames must be explained. In a conventional AFPM motor frame design, magnet rings are fixeted on the rotor discs. The rotor discs are connected to the shaft through one pair of bearings: one bearing on each side of the stator. The stator is fixed to the shaft through a flange. Each rotor disc must have two surfaces with a strict tolerances (surface, dimension, parallelism and cocentricity see technical drawing): one for the other rotor disc and one for the bearing

(see figure A.2). When assembling the motor, a set consisting of one rotor disc with bearing and shaft can be easily mounted but when the second second of a rotor disc with bearing must mounted things get difficult. It is practically impossible to mount a bearing on a shaft and inset it in a hole without damaging the bearing: balls inside the bearing push against the bearing rings and leave damage. Unless assembly is done with ultimate precaution expensive bearing can be destroyed.

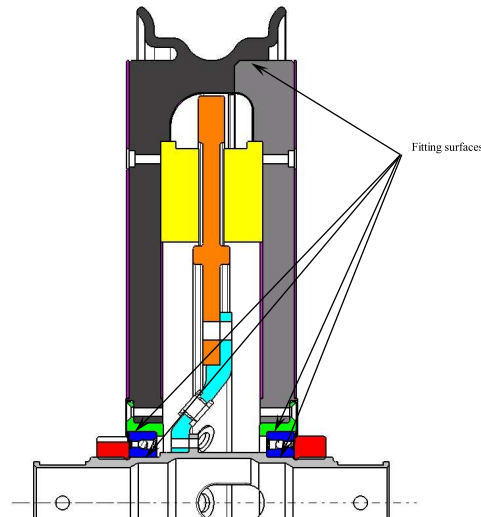


Figure A.2: Fitting surfaces in a conventional AFPM motor

For the CM, two different concepts were worked out. The first one is based on the Aurora design as shown in [3],[5] and in figure A.3. The aurora team motor frame design was purchased and used as inspiration for a Nuna conventional design. Many changes were made on the aurora design so that the motor comply with design philosophy of of the Nuna team. For example: hybrid spindle bearing are used in place of standard groove ball bearing, the width of the motor is reduced from 110mm to just 70mm, etc. The second concept is a new concept which differs a lot from the Aurora design. The description of the designs is given in the following section.

A.3.1 Description of the designs

The first design (Aurora design) is inspired by the Aurora solar team design. The magnet rings are placed on two discs. The rotor assembly rotates around the stator-shaft-flange assembly. The bearing between the rotor part and the stator part is a set of two spindle hybrid bearing from INA FAG. Each bearing is placed in a special bearing sleeve in one rotor disc.

The second design (Nuna Design) is completely new and offers many advantages that the design of Aurora design lacks. The rotor assembly of the motor consists of magnet rings mounted on a disc and a large ring called motor cover. The stator consists again of a shaft, a flange and the windings. The bearing in this concept is double row angular

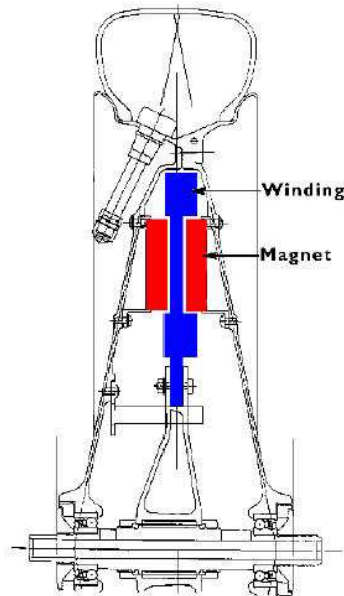


Figure A.3: Csiro original design made in 1996 [3]

contact ball bearings placed between the shaft and the rotor disc. There is in this way no contact between the motor cover and the bearing unit. no bearing damage is possible during assembly or dismantling the motor.

A.3.2 FEM analysis

In an axial flux permanent magnet motor a strong attractive magnetic force exists between the permanent magnet rings. In the case of Csiro this force is equal to 4.96kN with an airgap of 1.75mm and 5.54kN with 1mm airgap. Finite element analysis were conducted in order to optimize the design with safety factor of 1.5.

For ease of production, aluminum 7075 T6 chosen for the prototype of both designs. However, the final Csiro race motor would be a combination of magnesium and carbon. A new round of FEM analysis is then needed to optimize the design.

The most important factor in the design of the frame is the deflection of the magnet rings mounting covers. The magnet rings must in all time be mounted parallel in order to create a uniform magnetic field. This is a critical issue in the new proposed design. On the open side of the motor, the cover is only supported on the outer radius. The inner radius will be pulled towards the other magnet ring. In a worst case scenario the magnet rings will not be parallel anymore and the magnet flux won't be constant anymore. As a result, the performance of the motor will be negatively affected. In the prototype version, the motor cover is over engineered to avoid this problem.

The result of the FEM analysis are shown in figure A.4. Both Von Mises stress and the displacements are shown. The stresses (23.4MPa) are below the maximum allowed stress

(80MPa) in Aluminum. The maximum deflection is 0.077mm with an airgap of 1mm and a magnetic attractive force of 6kN. It should be mentioned that in the motor was not designed for the airgap of 1mm. But after the first tests with the motor, it was decided to test the airgap of 1mm to see what the influence of airgap reduction on the performance would be.

The maximum displacement of 0.077mm might seem large when compared to the airgap however, this is acceptable for two reasons. First, the deflection at the magnets is much smaller around the magnet rings. Second, the magnets rings add stiffness to the assembly through steel backing plates. The steel backing plates of the magnet rings were not taken into the analysis. Measurements showed that the distance between the mounted rings is uniform and that displacement is less than 0.04mm.

FEM analysis of the aurora design were also made. In figure A.5 the results of FEM analysis of the motor cover, the shaft and the flange are shown. The rotor sides were analyzed for the magnetic force results are shown in figure A.5(a) and A.5(b), the shaft for the bump load (see figure A.5(a) and A.5(b)) and the stator mounting flange for the maximum torque produced by the motor (see figure A.5(e) and A.5(f)) . This motor was also built in Nuna4 as shown in figure A.6 and tests were conducted with this motor on the track of RDW in Lelystad.

A.4 Comparison between Nuna and Aurora designs

It is important to make a comparison between both design in order to make a choice for the design that will be used in the car during the race. Not only the advantages of the Nuna design are discussed but also an efficiency test comparing both designs.

A.4.1 Advantages of the Nuna design

The difference between both design becomes obvious when the assembly procedure is discussed in table A.1. The Nuna concepts offers many advantages in comparison to the Aurora concept. Some of those are obvious from the assembly procedure. Here below a summation of the important advantages:

- Lower rotor weight due to the donut shape rotor cover instead of a rotor disc.
- Ease of assembly at least with 2 steps less. the chance of damaging the bearing is very much reduced as the attractive force between has no possibility to influence the assembly of the bearing.
- Offer the possibility of inspecting the stator cables without the need of dismantling the motor.
- Better cooling: The motor can be left partially open on the donut shaped rotor cover. This will be more obvious during testing.

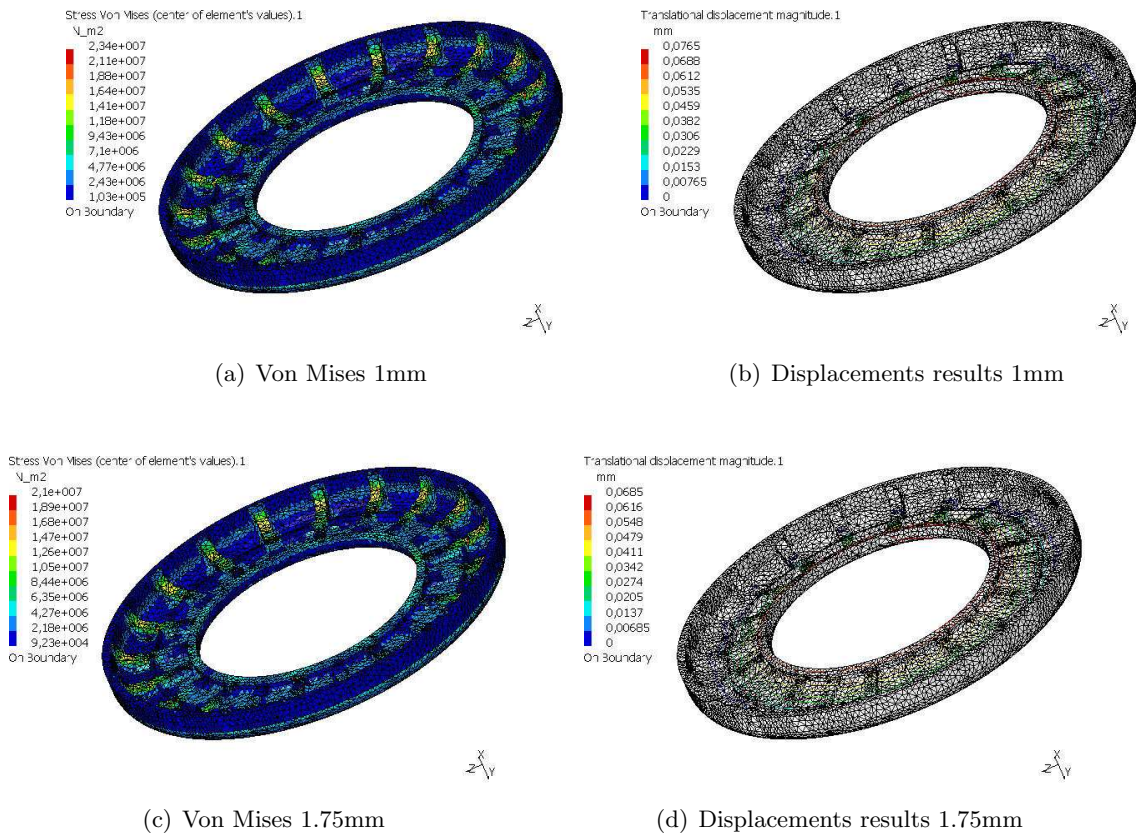
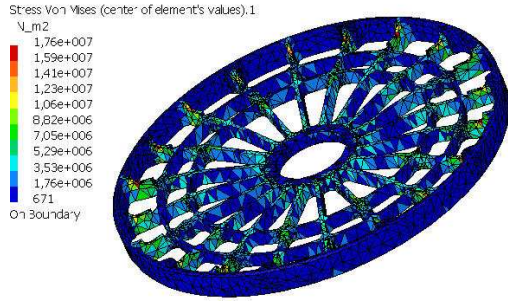
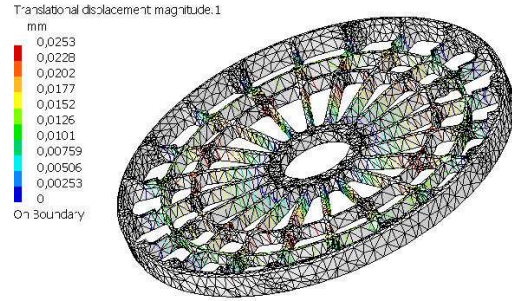


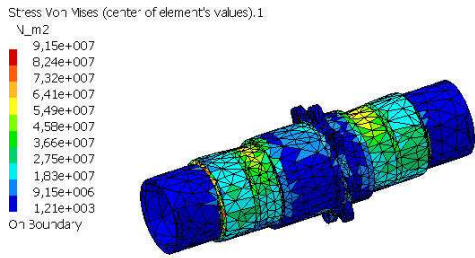
Figure A.4: FEM results for the motor cover for both 1mm and 1.75mm airgap.



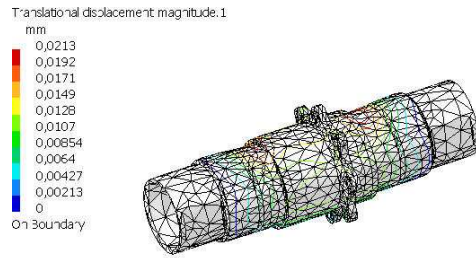
(a) Rotor Von Mises 1.75mm



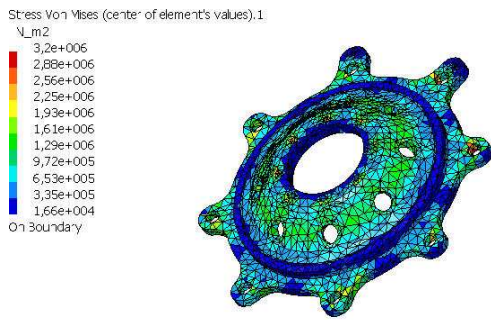
(b) Rotor displacements 1.75mm



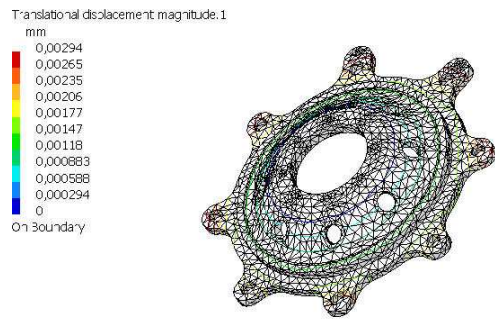
(c) Shaft Von Mises bump load



(d) Shaft displacements bump load



(e) stator flange von mises stress maximum torque



(f) stator flange displacements maximum torque

Figure A.5: FEM results for the motor rotor, stator mounting flange and shaft of aurora concept with 1.75mm airgap.

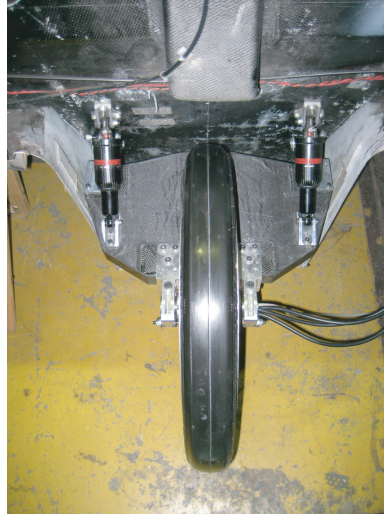


Figure A.6: Csiro built in Nuna4

A.4.2 Comparison test

The mechanical advantages of the new design are not enough to make a choice for the final frame design. Therefore, testing will make it clear which frame design is better. The efficiency of the motor was both tested for the speeds of 800-900-1000-1100 rpm while varying the torque between 12 and 21Nm with a step of about 1,5Nm. The results of those tests are shown here below in figure A.7.

- **At low torque:** All the results show that at low torque the efficiency of the conventional design is slightly higher but as the torque increases the efficiency difference becomes in the favor of the new design. The new design is on average 0.5% more efficient. This can be easily explained. At low torque, the dominant losses in the motor are the bearing losses as shown later appendix C. They count up 35% of the losses. The new design is fitted with the ZLKF20 bearing. It is a double row angular groove ball bearing with an angle of 60° . This bearing is actually not suitable for this type of application; this was however discovered after the motor was actually made and assembled. In the conventional design 2 hybride (ceremic balls) spindle bearings are used. Those are the most efficient bearing available. Therefore at low torque where the rotational losses are sort of dominant, both design have equal efficiency.

- **At high torque:**

The copper losses becomes larger and more dominant in the losses scheme. The temperature measurements showed that the conventional design reaches much higher temperatures up to 12° in comparison as shown in table A.2. The Nuna concept have therefore lower copper losses and a result higher efficiency.

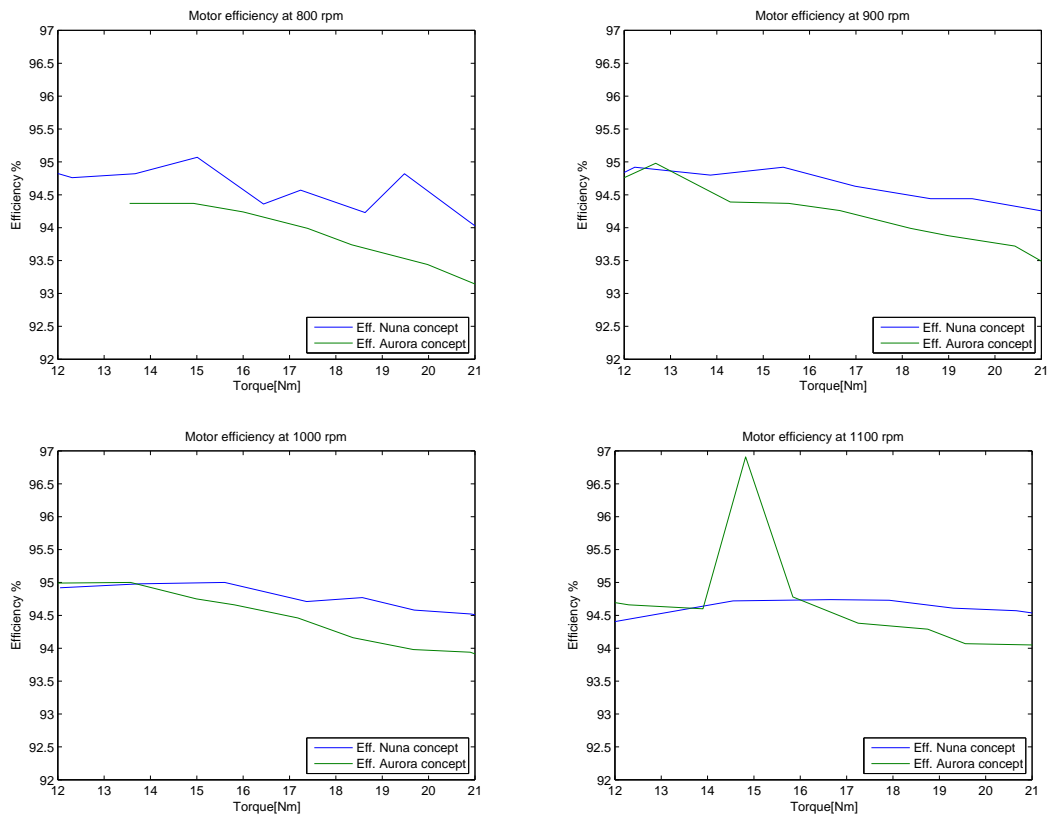


Figure A.7: Efficiency comparison between Nuna and Aurora concept

Table A.1: Assembly procedure comparison between the proposed motor frame1

Motor assembly steps		
	Aurora design (modified)	Nuna Concept
1	-Mount magnet ring on rotor disc	-Mount magnet ring on rotor disc
2	-Insert bearing in sleeve	-Insert shaft in bearing
3	-Insert bearing and sleeve in rotor discs	- - - - -
4	-Mount stator on flange and shaft	-Mount stator on flange and shaft
5	-Mount stator assembly the rotor disc with special tools	-Mount stator assembly to rotor disc with 4 M6 bolts
6	-Connect power cables to terminals on flange and than to three cables throughout the shaft	-Connect stator cable to terminals on the flange . power cables go straight of the motor opening
7	-Mount the second rotor disc. care must be given to this step. a mis-alignment can damage the bearing. after this step no cabling change is possible	-Mount the rotor donut disc to the rest. Due to its opening cables are still accessible

A.5 Conclusion

Based on the assembly and production benefits and the results of the comparison tests, it was chosen to continue testing with the newly proposed design with the centrally placed bearing. With this motor a series of test were conducted in order compare CM with BM.

In table A.3 the components of the housing, their function and the material used for fabrication are given.

Table A.2: Motor temperature in degree Celsius rise during testing

Motor temperature		
	Aurora concept	Nuna Concept
800	28.1-37.7	35.3-49.4
900	29.6-38.8	36.4-49.8
1000	29.9-39.5	35.2-49.4
1100	31.1-37.3	38.4-49.4

Machine part	Material	Proprieties
Shaft	42CrMo4	High strength
ZKLF20 Bearing INA FAG		pre-load adjustable
AM20 precision locknut INA FAG	steel	tensioning the bearing
Rotor	ALU 7075 T6	high thermal conductivity and strength
(40x)M4x10mm - magnet rings fixation	RVS 316	Din912-non magnetic ease of assembly
(10x)M0x20mm - stator fixation	RVS 316	Din912-non magnetic ease of assembly
(20x)M5x12mm - stator fixation	RVS 316	Din914-non magnetic ease of assembly
air valve	Aluminum	non magnetic ease of assembly

Table A.3: Motor components

Appendix B

Test Setup measurements

Since the CM is a special design for a special application finding a test setup was not possible. Therefore, a custom setup was needed in order to measure the efficiency of the Csiro drive. Not only a custom test setup was needed, the test procedure was very important and had to be done with a lot of care. The start up of a test for example is crucial; any mistake in the order of turning on the machinery can cause damage to the equipments the motor had to be brought slowly into its voltage. Another example is regenerative braking of the tested motor, switching the throttle to the regenerative mode could have destroyed the motor controller. In the appendix the test setup and test procedures are described.

B.1 Test setup

The test setup consist of 2 parts: the motor side and the load side. Between the motor and the load a torque sensor is placed (see figure B.3) to measure the torque delivered by the motor. Electric power is fed to the motor through three power supplies (see figure B.1) and inverter also known as motor controller. The power input and output of the motor controller is measured by power analyzer (see figure B.2). Sadly this was the limiting factor of the tests. The maximum allowed current through this power analyzer was 20A. This value limited the maximum torque that was tested (22Nm at 800rpm increasing 24Nm at 1100rpm). Luckily that was in the torque and speed range of Nuna during the race. On the motor side the speed is set and controlled by the motor controller software.

On the load side, generated power is dissipated in a large heating unit. The heating unit consist of a large variable resistance (see figure B.6). The torque was defined by the value of the resistance. The load was also connected to a motor controller and laptop. The laptop had a monitoring function such as temperature monitoring of the stator and velocity check. 3 extra small power supplies were used: 2 for the motor controllers and one for the torque sensor. The layout of the test setup is shown in figure B.7 and figure B.5. The components used in the test set are listed in table B.1:

Table B.1: Equipments used during testing.

	Device	Function	Model
Electrical	3 large DC power supply	Stable, variable DC voltage, power supply	Delta electronics SM70-22
	2 small DC power supply	Power supply for torque sensor	Delta electronics E 030-1 ES 030-2
	Power analyzer	Electric power measurements	Yokogawa PZ4000 fig.B.2
	Variable resistance	power discharge generated by load	Smit Slikkerveer fig.B.6
	2 laptops	Control and data logging	HP nc 8430
	2 motor controllers	Control of motor and load	Tritium WaveSculptor figB.4
	1 circuit breaker/glow circuit	Slowly bring the motor under the desired voltage	self-made
Mechanical	2 couplings	Motor/load connection to toque sensor	Lorenz 950-300 fig.B.3
	Torque sensor	Torque measurements	Lorenz dual torque sensor DR-2412R fig.B.3
	Test Frame	Motor and load mounting	Custom design

B.2 Test condition and procedures

The performance measurements took place for the following operating conditions:

- DC-link bus voltage = 160V dc
- Torque = [10; 23] Nm with a step of about 0.75Nm
- Rotational speed = [800; 900; 1000; 1100] RPM

The procedure followed for these measurements is:

1. Adjust DC-link bus voltage to desired value 160V dc on the power supply as shown in figure B.1
2. Adjust the rotational speed to desired value through the controlling program delivered with Tritium controller
3. Go through the torque range by adjusting the load manipulating the DC generator anchor resistance. 2 steps turns on the variable resistance are roughly equal to 0.75Nm step.
 - Wait by each torque until speed of motor stabilize
 - Measuring time for each torque value is 4min: practical reasons
 - Turn on the averaging function of the power analyzer
 - Fill in the values of the average input powers into motor controller and motor
 - Turn off averaging and repeat previous steps
4. Repeat previous two steps until all desired speeds are measured.
5. Logging data in excel sheet:
 - fill in excel sheet log time start of the measurements for each speed and torques
 - Write DC-link bus voltage average in Volts. Average given by the power analyzer
 - Torque sensor output is directly logged and should be averaged later with a Matlab program
 - RPM of motor using the motor controller
 - Input current in Amperes. Average given by the power analyzer
 - Input Power of motor and motor controller (average by the power analyzer)
 - Begin and end temperature of both motor and load.

6. Repeat above procedure for all conditions

7. Perform the measurements for each speed twice

The results of such a measurement for one speed (1100rp,) are shown in table B.2

Table B.2: Measurements data for a 1100rpm test.

Data Csiro test 1100 rpm [10; 24] Nm															
t Start	t Stop	Stand	P_{in}	U_{3p}	I_{3p}	P_{3p}	τ_{mean}	P_{mech}	%controller	% m	% set	t_{ms}	t_{me}	t_{g-s}	t_{ge}
15:28:00	15:32:00	S3-4	1201	118,45	8,26	1167	9,66	1112,49	97,17	95,33	92,63	30,2	29,9	37,5	35,8
15:34:00	15:38:00	S4-1	1314	118,42	8,85	1279	10,56	1215,86	97,34	95,06	92,53	29,9	29,9	35,5	34,7
15:40:00	15:44:00	S4-3	1421	118,4	9,84	1383	11,43	1317,00	97,33	95,23	92,68	30	30,2	34,7	34,6
15:46:00	15:50:00	S4-5	1538	118,38	10,15	1497	12,39	1427,66	97,33	95,37	92,83	30,3	30,5	34,9	35,1
15:52:00	15:56:00	S5-2	1636	118,36	10,74	1594	13,22	1522,69	97,43	95,53	93,07	30,6	30,9	35,3	35,7
15:58:00	16:02:00	S5-4	1746	118,32	11,37	1701	14,12	1626,80	97,42	95,64	93,17	31	31,3	36,1	36,6
16:04:00	16:08:00	S6-1	1853	118,26	11,98	1805	14,99	1726,80	97,41	95,67	93,19	31,4	31,8	37	37,7
16:10:00	16:14:00	S6-3	1952	118,25	12,56	1904	15,79	1819,25	97,54	95,55	93,20	32	32,3	38,2	38,8
16:16:00	16:20:00	S6-5	2060	118,22	13,21	2009	16,68	1921,09	97,52	95,62	93,26	32,5	32,9	39,3	40,2
16:28:00	16:32:00	S7-4	2250	118,11	14,34	2196	18,21	2098,54	97,6	95,56	93,27	33,6	34	41,9	43
16:34:00	16:38:00	S8-1	2348	118,11	14,92	2292	19,01	2189,71	97,62	95,54	93,26	34,2	34,6	43,6	44,5
16:40:00	16:44:00	S8-3	2438	118,08	15,46	2382	19,75	2274,77	97,70	95,5	93,30	34,9	35,2	45,2	46,1
16:46:00	16:50:00	S8-5	2539	118,05	16,07	2481	20,56	2368,68	97,72	95,47	93,29	35,5	35,9	46,8	47,9
16:52:00	16:56:00	S9-2	2628	118	16,59	2568	21,26	2449,24	97,72	95,38	93,2	36,2	36,6	48,7	49,7
16:58:00	17:02:00	S9-4	2721	117,95	17,17	2658	22,03	2537,41	97,69	95,46	93,25	36,9	37,3	50,5	51,7
17:04:00	17:08:00	S10-1	2811	117,92	17,69	2748	22,73	2618,37	97,76	95,28	93,15	37,5	37,9	52,3	53,5
17:10:00	17:14:00	S10-3	2897	117,9	18,21	2833	23,41	2697,21	97,79	95,21	93,10	38,3	38,7	54,3	55,5
17:16:00	17:20:00	S10-5	2991	117,85	18,78	2925	24,17	2783,79	97,79	95,17	93,07	39	39,5	56,4	57,8



Figure B.1: 3 Delta electronics for power supply.

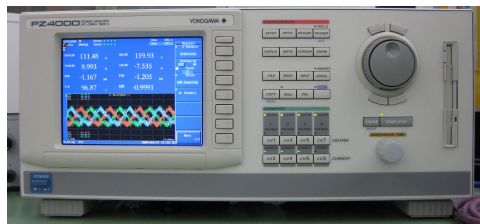


Figure B.2: Power analyzer Yokogawa PZ4000 DC twoMHz 5MS/s.

B.3 Results

During testing there was three sources of data: torque from the torque sensor, velocity and temperature from the motor controller and power from the power analyzer. From all these data only the torque data had to be processed. The other data value were given straight on the laptop or the power analyzer screens and were overwritten manually into an excel sheet.

For each tested speed, the torque was increased from 10 to 24Nm with a step of about 0.8Nm. The test was continuous and lasted nearly two hours. This meant that the torque data file was very large (frequency 100Hz). The time start of each tested set point was written down. In this way, there was a main start time of a test and sub starting points for the torques. An example is given here below for the 900rpm in table B.3. The Torque data file was cut in Matlab and into smaller intervals in which the efficiency of the motor was calculated. An example of the torque is given in figure B.8. The complete set of results of the testing is given in several tables in the excel sheet file.

Table B.3: Time intervals during testing at 900 rpm

Timeline 900 rpm									
Start	11:30:30	11:36:15	11:42:45	11:48:45	11:54:45	12:00:45	12:06:50	12:13:45	12:19:45
End	11:34:30	11:40:15	11:46:45	11:52:45	11:58:45	12:04:45	12:11:40	12:17:45	12:23:45

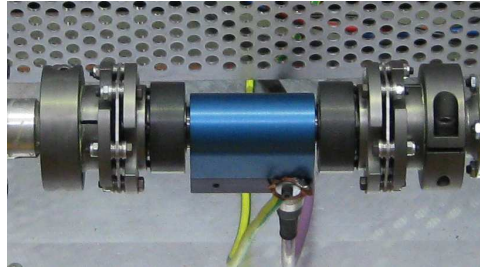


Figure B.3: Torque sensor en couplings assembly.



Figure B.4: Motor controller Tritium WaveSculptor.

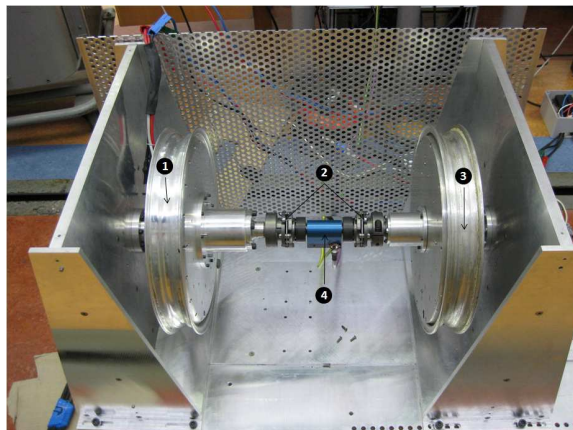


Figure B.5: Side view Mounting frame of the motor and load



Figure B.6: Variable Resitance

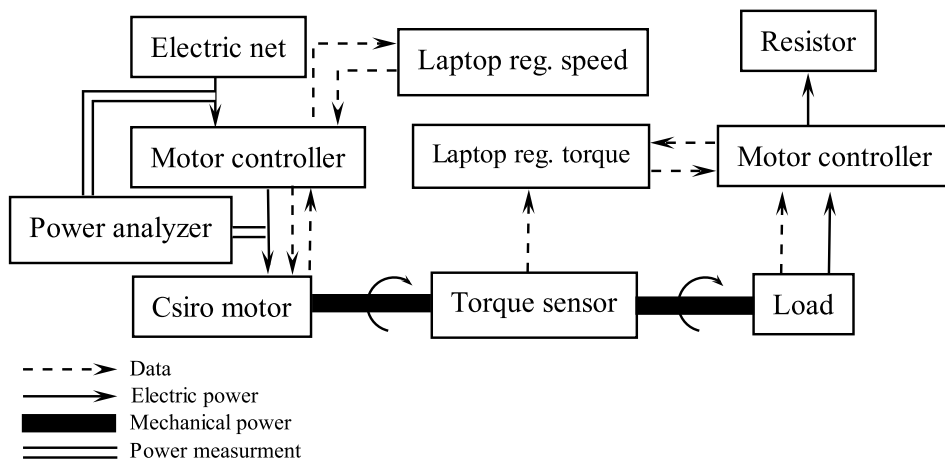


Figure B.7: Connection diagram of the test setup equipments.

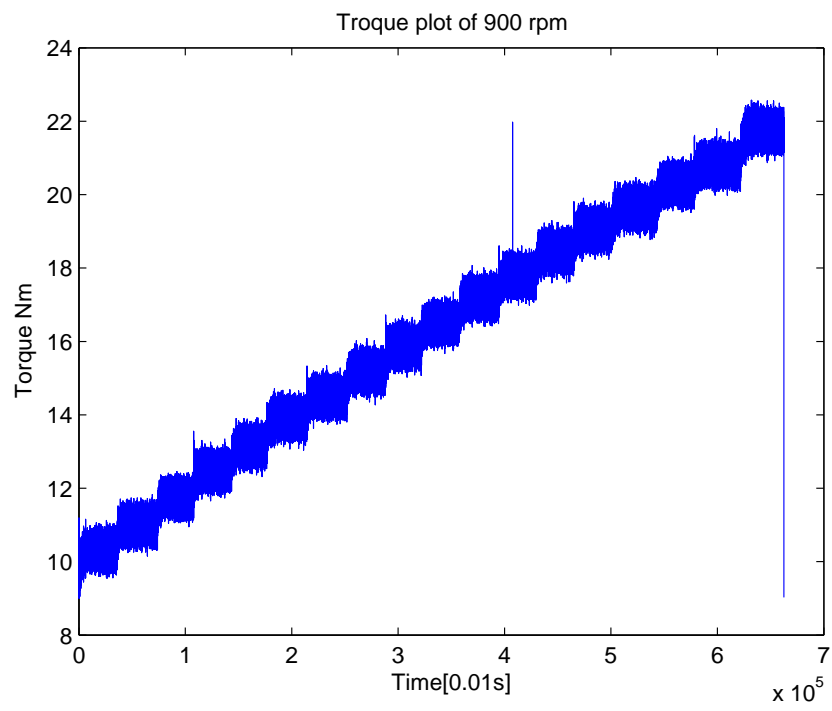


Figure B.8: Torque plot of 900 rpm

Appendix C

Model evaluation

C.1 Introduction

Modeling the Csiro motor is not only important to understand its efficiency but also to separately qualify and quantify the losses in order to optimize the drive. In the case of the csiro, improvements are possible mechanically in the design of the motor frame and electrically in the inductors. In this section of the appendices, the influence of each loss is shown and calculated and when possible compared to what was measured during testing.

C.2 Influence of each loss

Figure C.1 shows the influence of each loss discussed above.

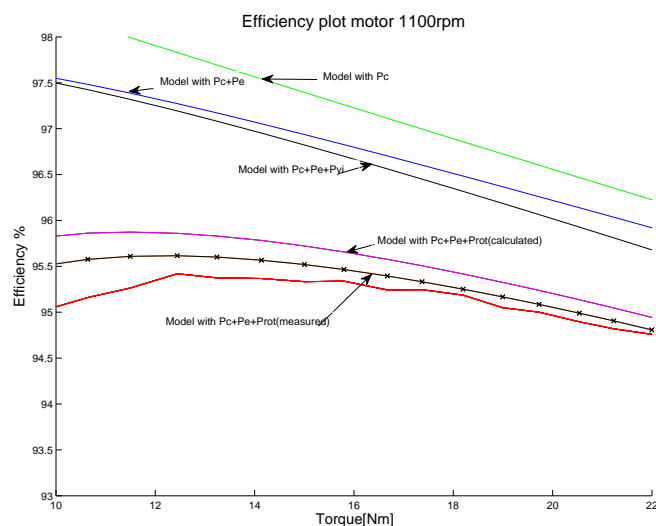


Figure C.1: Influence of each loss on the model curve (1000rpm)

Table C.1: Influence on the mechanical losses

1000RPM- $BL_{1000} = 16.7[W]$, $WL_{1000} = 2.2[W]$						
Total losses [W]	CL [W]	CL %	RL %	YL [W]	YL %	ECL %
47,5	21,6	44,4	39,8	0,6	1,2	14,6
51,3	25,5	48,2	36,8	0,8	1,5	13,5
55,3	29,5	51,6	34,1	0,9	1,7	12,5
59,3	33,5	54,6	31,8	1,1	1,9	11,7
64,1	38,3	57,6	29,5	1,4	2,1	10,8
68,4	42,6	59,9	27,6	1,6	2,3	10,1
73,4	47,6	62,3	25,7	1,9	2,6	9,4
78,3	52,5	64,2	24,1	2,2	2,8	8,9
83,3	57,5	66,0	22,7	2,5	3,0	8,3
89,0	63,2	67,8	21,2	2,9	3,2	7,8
94,2	68,4	69,2	20,1	3,2	3,4	7,4
100,1	74,3	70,6	18,9	3,6	3,6	6,9
106,1	80,3	71,8	17,8	4,1	3,8	6,5
111,8	86,0	72,9	16,9	4,5	4,0	6,2
118,5	92,6	74,0	15,9	5,0	4,2	5,9
124,1	98,3	74,8	15,2	5,5	4,4	5,6
130,7	104,9	75,7	14,5	6,0	4,6	5,3

This graph shows that the influence of the mechanical design is large. For example, the copper losses at 1000 rpm varies from 21.6 to 104.9W with a torque varying from 10.1 to 22Nm. The rotational losses are 18.9W ($WL=2.2W$ and $BL=16.9W$) calculated with model and 25.52W measured. It is than obvious that the rotational losses are very important and must be taken into consideration. The influence of the rest of the losses are shown in figure C.1.

In [3] the efficiency is given to be 97.5% but without taking the mechanical losses into consideration. This explains the difference between measured efficiency and specified efficiency by the manufacturer.

Measured	Calculated
16.7	14.61
20.7	16.7
25.5	18.9
30.8	21.2

Table C.2: Comparison of measured and calculated rotational losses

The difference between the measured and calculated rotational losses is expected as the equations used are an approximation. A different approach can be used to get a better calculation of the rotational losses. The bearing losses are proportional to the rotational speed whereas the windage losses are proportional to the rotational losses to the third

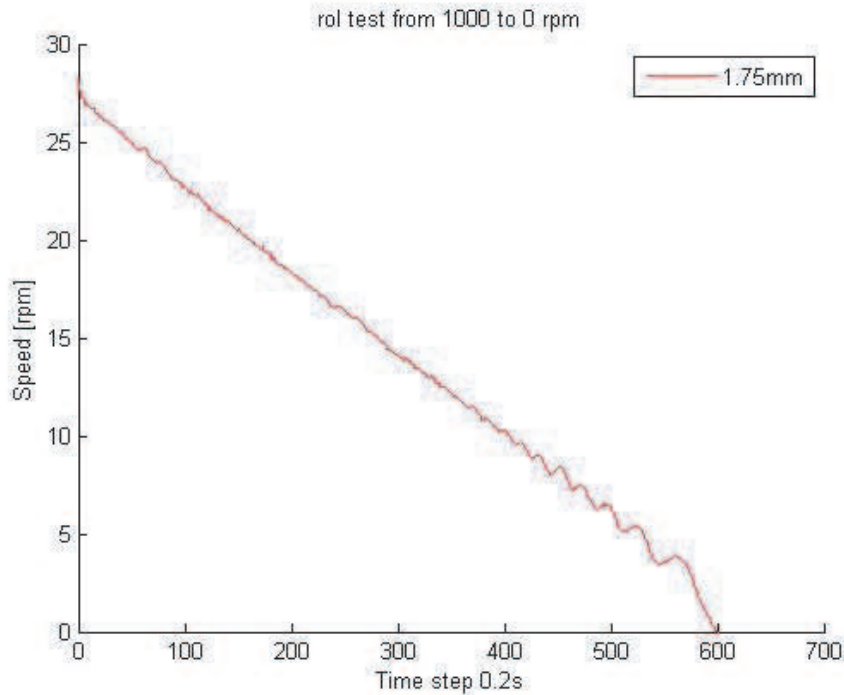


Figure C.2: Rol test from 28rpm to 0

power. A small part of a roil test is shown in figure C.2. The test was made with a fake stator just to have influence of the rotational losses. An example of such a test is given in figure 13 of the paper. Just at the end of the test, the influence of the windage becomes ignorable. The speed curves becomes a straight line. From this line the deceleration caused by the bearing internal friction can be calculated. It is equal to the slope of the line. From the deceleration, the negative torque caused by the bearing can be calculated.

Knowing the formula of the bearing losses, windage losses formula can be derived.

This method has one disadvantage, any change in the bearing pre-tension means that the formula isn't valid anymore. Another important point is that when the motor will be built in the car, the bearing losses will become larger as the weight of the vehicle causes more friction in the bearing. This is in the scope of this thesis not important because the comparison is made with another motor that was also bench tested.

C.3 Conclusion

The results of the model showed the rotational losses are very important and must not be neglected. This explains the difference between the measured efficiency and the efficiency given by the manufacturer.

Appendix D

Matlab files

In this appendix the matlab files created and used in the thesis are given.

D.1 MatlabAnalyzing torque data and computing efficiencies

```
%Processing the torque data and computing the efficiencies of the motor 1
clear all
close all
clc 6

for loop=1:2,
%loading data from both experiments at 900rpm
if loop==1, 11
    file =load('torquedata900_2.txt');%xlsread('torquedata900_2_b ');%
    t_s= load('ts_900_2.txt');
    timem = load('t_900_2.txt')
    p=load('p_900_2.txt');
else, 16
    file = load('torquedata900_3.txt');%xlsread('torquedata900_3_b ');
    t_s= load('ts_900_3.txt');
    timem = load('t_900_3.txt')
    p=load('p_900_3.txt');
end 21

%giving the start time from time vector
starth= t_s(1);
startm= t_s(2);
starts= t_s(3); 26
%-----%

tel=0;
telh=starth;
telm=startm; 31
tels=starts;

h = starth;
m = startm;
s = starts; 36

%defining the time of each torque data set
for i=1:size(file,1)

    if(telh<23) 41
        if(telm<59)
            if(tels<59)
                if(tel<99)
                    file(i,2) = h;
                    file(i,3) = m;
                    file(i,4) = s;
                    tel = tel+1; 46
```

```

else
    file(i,2) = h;
    file(i,3) = m;
    file(i,4) = s;
    tel = 0;
    s = s + 1;
    tels = tels + 1;
end
51

else
    if (tel < 99)
        file(i,2) = h;
        file(i,3) = m;
        file(i,4) = s;
        tel = tel + 1;
    else
        file(i,2) = h;
        file(i,3) = m;
        file(i,4) = s;
        tel = 0;
        % s = s + 1;
        % tels = tels + 1;
        tels = 0;
        s = 0;
        m = m + 1;
        telm = telm + 1;
    end
    end
56

else
    if (tels < 59)
        if (tel < 99)
            file(i,2) = h;
            file(i,3) = m;
            file(i,4) = s;
            tel = tel + 1;
        else
            file(i,2) = h;
            file(i,3) = m;
            file(i,4) = s;
            tel = 0;
            s = s + 1;
            tels = tels + 1;
        end
    else
        if (tel < 99)
            file(i,2) = h;
            file(i,3) = m;
            file(i,4) = s;
            tel = tel + 1;
        else
            file(i,2) = h;
            file(i,3) = m;
            file(i,4) = s;
            tel = 0;
            % s = s + 1;
            % tels = tels + 1;
            tels = 0;
            s = 0;
            % m = m + 1;
            % telm = telm + 1;
            telm = 0;
            m = 0;
            h = h + 1;
            telh = telh + 1;
        end
    end
    end
51

end
121

else
    file(i,2) = h;
    file(i,3) = m;
    file(i,4) = s;
    telh = 0;
    h = 0;
end
126

end
131

%%%%%%%%%%%%%%%%%%%%%%%%%%%%%%%%%%%%%%%%%%%%%%%%%%%%%%%%%%%%%%%%%%%%%%%%
%loading motor rotational speed vector

```

D.1. MATLABANALYZING TORQUE DATA AND COMPUTING EFFICIENCIES_{xxix}

```

s=900; %motor speed [rpm]

%setting the torque limits to remove the zero value placed in place of the
%timeout error s
grensonder =0;
grensboven =50;

%calculating the torque average
m=[];
for j=1:length(timem);
startmeeth = timem(j,1);
startmeetm = timem(j,2);
startmeets = timem(j,3);
stopmeeth = timem(j,4);
stopmeetm = timem(j,5);
stopmeets = timem(j,6);

startmeet = (10000*startmeeth) + (100*startmeetm) + startmeets;
stopmeet = (10000*stopmeeth) + (100*stopmeetm) + stopmeets;

select=[];

for i=1:size(file,1)
filetime = (10000*file(i,2)) + (100*file(i,3)) + file(i,4);

if(filetime>=startmeet && filetime<=stopmeet)
if(file(i,1)> grensonder && file(i,1)<grensboven)
if isempty(select)
select = file(i,:);
else
select = [select;file(i,:)];
end
end
end

end;

% figure
% plot(select(:,1))

%calculating the set efficiency
eff_controller(j,1)=p(j,2)/p(j,1)*100;

% de torque file is
T=(select(:,1))

% TT=T(find(T~=0));

% mean(T)
% mean(TT)
% length(T)
% length(TT)

plot(select(:,1))
pause
% de gemiddelde waarde van de torque
m(j,1)=mean(T)

% Calculating standard deviation
st(j,1)=std(T)

%calculating the mechanical power
pmech(j,1)=pi/30*s*m(j)

%error cal for the error bar
%E(j,1)=st(j,1)/m(j,1)*pmech(j,1)/p(j,2)

%Error in mechanical power calculation
E(j,1)= st(j,1)/m(j,1)*100

effmotor(j,1)=pmech(j,1)/p(j,2)*100

eff(j,1)=eff_controller(j,1)*effmotor(j,1)/100

%tmean=[tmeam;m(j)]
end

%save the data generated
vec=[eff_controller effmotor eff]

```

```

figure(1);
hold on
xlabel('Torque [Nm]')
ylabel('Efficiency %')
title('Efficiency plot motor/controller/set')
plot(m,vec(:,1),'r', m,vec(:,2), 'm', m,vec(:,3), 'b')
legend('eff. controller','eff. motor','eff. set',2);
% errorbar(m,vec(:,2),E)
pause;
clear all

end

```

D.2 MatlabPlotting the results of all speeds and torques

```

%%loading and plotting efficiency results for all speeds and torques

close all
clear all
clc

for loop=1:4,
if loop==1,
s=800;

vec2=load('eff800_2.txt');
tor2=load('gemptorque800_2.txt');

vec3=load('eff800_3.txt');
tor3=load('gemptorque800_3.txt');

length(vec2)
length(vec3)
vec= (vec2(1:17,:)+vec3(1:17,:))/2;
tor= (tor2(1:17,:)+tor3(1:17,:))/2;

%defining error bar
% E= abs(vec2-vec3)
% M= max(vec(:,2))

figure(1);
hold on
xlabel('Torque [Nm]')
ylabel('Efficiency %')
title('Efficiency plot motor/controller/set 800rpm')
plot(tor,vec(:,1),'-r', tor,vec(:,2), '-m', tor,vec(:,3), '-b');% , tor,N, 'g')
plot(tor2(1:17),vec2(1:17,1),'xr', tor2(1:17),vec2(1:17,2),'xm', tor2(1:17),vec2(1:17,3),'xb')
plot(tor3(1:17),vec3(1:17,1),'.r', tor3(1:17),vec3(1:17,2), '.m', tor3(1:17),vec3(1:17,3), '.b')
legend('Eff. controller','Eff. motor','Eff. set',4);
axis ([10 20 91 98])

elseif loop==2
s=900;
vec2=load('eff900_2.txt');
tor2=load('gemptorque900_2.txt');

vec3=load('eff900_3.txt');
tor3=load('gemptorque900_3.txt');

length(vec2)
length(vec3)
vec= (vec2(1:18,:)+vec3(1:18,:))/2;
tor= (tor2(1:18,:)+tor3(1:18,:))/2;

figure(2);
hold on
xlabel('Torque [Nm]')
ylabel('Efficiency %')
title('Efficiency plot motor/controller/set 900rpm')
plot(tor,vec(:,1),'-r', tor,vec(:,2), '-m', tor,vec(:,3), '-b');% , tor,N, 'g')
plot(tor2(1:18),vec2(1:18,1),'xr', tor2(1:18),vec2(1:18,2),'xm', tor2(1:18),vec2(1:18,3),'xb')
plot(tor3(1:18),vec3(1:18,1),'.r', tor3(1:18),vec3(1:18,2), '.m', tor3(1:18),vec3(1:18,3), '.b')

```

```

        legend('Eff. controller','Eff. motor','Eff. set',4);
        axis ([10 22 91 98])
    elseif loop==3
        s=1000
        vec2=load('eff1000_3.txt');
        tor2=load('gemptorque1000_3.txt');

        vec3=load('eff1000_4.txt');
        tor3=load('gemptorque1000_4.txt');

        length(vec2)
        length(vec3)
        vec= (vec2(1:17,:)+vec3(1:17,:))/2;
        tor= (tor2(1:17,:)+tor3(1:17,:))/2;

    figure(3);

        hold on
        xlabel('Torque[Nm]')
        ylabel('Efficiency %')
        title('Efficiency plot motor/controller/set 1000rpm')
        plot(tor,vec(:,1),'-r', tor,vec(:,2), '-m', tor,vec(:,3), '-b');% tor,N, 'g')
        plot(tor2(1:17),vec2(1:17,1),'xr', tor2(1:17),vec2(1:17,2),'xm', tor2(1:17),vec2(1:17,3),'xb')
        plot(tor3(1:19),vec3(1:19,1),'r', tor3(1:19),vec3(1:19,2), '.m', tor3(1:19),vec3(1:19,3), '.b')
        legend('Eff. controller','Eff. motor','Eff. set',4);
        axis ([10 23 91 98])

    else
        s=1100;
        vec1=xlsread('vec1100_2');
        tor1=vec1(:,1);
        length(vec1)

        vec2=xlsread('vec1100_3');
        tor2=vec2(:,1);

        length(vec2)

        %chekking length

        vec= (vec1(1:17,2:4) + vec2(1:17,2:4))/2;
        tor= (tor1(1:17,:) + tor2(1:17,:))/2;

        figure(4);
        hold on
        xlabel('Torque[Nm]')
        ylabel('Efficiency %')
        title('Efficiency plot motor/controller/set 1100rpm')
        plot(tor,vec(:,1),'-r', tor,vec(:,2), '-m', tor,vec(:,3), '-b');% tor,N, 'g')
        plot(tor1(1:17),vec1(1:17,2),'xr', tor2(1:17),vec1(1:17,3), 'xm', tor1(1:17),vec1(1:17,4), 'xb')
        plot(tor2(1:17),vec2(1:17,2),'r', tor2(1:17),vec2(1:17,3), '.m', tor2(1:17),vec2(1:17,4), '.b')

        legend('Eff. controller','Eff. motor','Eff. set',4);
        axis ([10 23 91 98])

    end

    pause
    clear all
    clc
    end
end

```

D.3 MatlabModel and plot with measured data

```

%%%plotting the test results for all speeds%%%%%%%%%%%%%%%%%%%%%%%%%%%%%%%%%%%%%%%%%%%%%%%%%%%%%%%%%%
%
%loading data
clear all
close all
clc
clf

for loop=1:4,

```

```

if loop==1,
    s=800;

    vec2=load('eff800_2.txt');
    tor2=load('gemtorque800_2.txt');
    tw2=load('tw800_2.txt');
    kt2=load('kt800_2.txt');

    vec3=load('eff800_3.txt');
    tor3=load('gemtorque800_3.txt');
    tw3=load('tw800_3.txt');
    kt3=load('kt800_3.txt');

    length(vec2)
    length(vec3)
    vec= (vec2(1:17,:)+vec3(1:17,:))/2;
    tor= (tor2(1:17,:)+tor3(1:17,:))/2;
    tw= [29.6535; 30.4099; 31.4878; 32.7111; 33.9081; 35.0634; 36.5014; 37.8054;
        39.2447; 40.7794;
        42.2505; 44.0115; 45.5296; 47.1975; 48.9323; 50.5692; 52.0000] %(tw2(1:17,:)+
        tw3(1:17,:))/2;
    %kt= (kt2(1:17)+kt3(1:17))/2;
    %kt=1.1655;
    length(tw)

    %defining error bar
    E= abs(vec2-vec3)

elseif loop==2
    s=900;
    vec2=load('eff900_2.txt');
    tor2=load('gemtorque900_2.txt');
    tw2=load('tw900_2.txt');
    kt2=load('kt900_2.txt');

    vec3=load('eff900_3.txt');
    tor3=load('gemtorque900_3.txt');
    tw3=load('tw900_3.txt');
    kt3=load('kt900_3.txt');

    length(vec2);
    length(vec3);
    vec= (vec2(1:18,:)+vec3(1:18,:))/2;
    tor= (tor2(1:18,:)+tor3(1:18,:))/2;
    % tw= (tw2(1:18,:)+tw3(1:18,:))/2;
    tw=[30.0089;
        31.1210;
        32.1791;
        33.3897; 34.5623;
        35.8009; 37.2234;
        38.5054; 40.0120;
        41.5425; 43.0381;
        44.7459; 46.2598;
        47.9913; 49.7083;
        51.3798; 53.3479; 53.3479 ]
    %kt= (kt2(1:18)+kt3(1:18))/2;
    %kt=1.1655;
    %defining error bar
    E= abs(vec2-vec3);

elseif loop==3
    s=1000
    vec2=load('eff1000_3.txt');
    tor2=load('gemtorque1000_3.txt');
    tw2=load('tw1000_3.txt');

    kt2=load('kt1000_3.txt');

    vec3=load('eff1000_4.txt');
    tor3=load('gemtorque1000_4.txt');
    tw3=load('tw1000_4.txt');
    kt3=load('kt1000_4.txt');

    length(vec2)
    length(vec3)
    vec= (vec2(1:17,:)+vec3(1:17,:))/2;
    tor= (tor2(1:17,:)+tor3(1:17,:))/2;
    %kt= (kt2(1:17,:)+kt3(1:17,:))/2;
    %kt=1.1655;
    %tw= (tw2(1:17,:)+tw3(1:17,:))/2;
    tw=[30.8787; 32.2806;
        33.7635; 35.2474;
        37.0239; 38.6268;
        40.5094; 42.3442;

```



```

kfb=1; % fricton coefficient of the bearing [m^2/s^2]
mr=4.92*2+7; % rotor mass [kg]
msh=1; % shaft mass [kg]
rev=60; % speed [rev/s]
Pb=0.06*kfb*(mr+msh)*rev; % bearing losses [W]

%%%%%%%%%%%%%%%%%%%%%%%%%%%%%%%%%%%%%%%%%%%%%%%%%%%%%%%%%%%%%%%%%%%%%%%%
%aerodymic losses
%determining the reynolds number
ro_air=1.2; % air density [kg/m3]
Rout=0.2026; % outer diameter [m]
Rsh=0.01; % shaft diameter [m]
v=2*pi*Rout*rev; % linear velocity of the outer diameter [m/s]
mu=1.8e-5; % dynamic viscosity of the air [Pa s]
Re= ro_air*Rout*v/mu;

cf=3.87/(Re)^0.5;

%windage losses
Pwind= 1/2*cf*ro_air*(2*pi*rev)^3*(Rout^5-Rsh^5) ;

%inductor losses
Pind=0.063*(i(j)^2);
%%%%%%%%%%%%%%%%%%%%%%%%%%%%%%%%%%%%%%%%%%%%%%%%%%%%%%%%%%%%%%%%%%%%%%%%
%EFFICIENCY CALCULATION

N(j)=Pout(j)/(Pout(j)+Pc(j)+Pe+ Pb+Pwind)*100;

% Pind(j)
end
% plotting the results
if loop==1,
figure(1);
hold on
xlabel('Torque [Nm]')
ylabel('Efficiency %')
title('Efficiency plot motor/controller/set 800rpm')
%plot(tor,vec(:,1),'r', tor,vec(:,2), 'm', tor,vec(:,3), 'b', tor,N, 'g')
errorbar(tor, smooth(vec(:,1)), E(:,1)/2,'r')
errorbar(tor, smooth(vec(:,2)), E(:,2)/2,'k')
errorbar(tor, smooth(vec(:,3)), E(:,3)/2,'b')
legend('eff. controller','eff. motor','eff. set','motor model',4);
axis ([10 20 91 98])

figure(2)
hold on
xlabel('Torque [Nm]')
ylabel('Efficiency %')
title('Efficiency plot motor 800rpm')
plot( tor,smooth(vec(:,2)), 'm', tor,N, 'g')
legend('Smoothed eff. motor','Model eff. motor',4);
axis ([10 20 93 98])

figure(3)
hold on
xlabel('Torque [Nm]')
ylabel('kt%')
title('kt plot at several torques')
%plot(tor, kt, 'r')
legend('800 rpm',4);
elseif loop==2,
figure(4);
hold on
xlabel('Torque [Nm]')
ylabel('Efficiency %')
title('Efficiency plot motor/controller/set 900rpm')
%plot(tor,vec(:,1),'r', tor,vec(:,2), 'm', tor,vec(:,3), 'b', tor,N, 'g')
errorbar(tor, smooth(vec(:,1)), E(:,1)/2,'r')
errorbar(tor, smooth(vec(:,2)), E(:,2)/2,'k')
errorbar(tor, smooth(vec(:,3)), E(:,3)/2,'b')
legend('eff. controller','eff. motor','eff. set','motor model',4);
axis ([10 22 91 98])

figure(5)
hold on
xlabel('Torque [Nm]')
ylabel('Efficiency %')
title('Efficiency plot motor 900rpm')
plot( tor,smooth(vec(:,2)), 'k', tor,N, 'g')
legend('Smoothed eff. motor','Model eff. motor',4);
axis ([10 22 93 98])

```

D.4. MATLABCOMPARISON BETWEEN CSIRO MOTOR AND SURFACE DRAW_{xxxxv}

```

figure(3)
hold on
%plot(tor, kt, 'b')
263

elseif loop==3,
figure(6);
hold on
xlabel('Torque [Nm]')
ylabel('Efficiency %')
title('Efficiency plot motor/controller/set 1000rpm')
%plot(tor,vec(:,1),'r', tor,vec(:,2), 'm', tor,vec(:,3), 'b', tor,N, 'g')
errorbar(tor, smooth(vec(:,1)), E(:,1)/2,'r')
errorbar(tor, smooth(vec(:,2)), E(:,2)/2,'k')
errorbar(tor, smooth(vec(:,3)), E(:,3)/2,'b')
legend('eff. controller','eff.motor','eff. set','motor model',4);
axis ([10 22 91 98])
268

figure(7)
hold on
xlabel('Torque [Nm]')
ylabel('Efficiency %')
title('Efficiency plot motor 1000rpm')
plot( tor,smooth(vec(:,2)), 'b', tor,N, 'g')
legend('Smoothed eff.motor','Model eff. motor',4);
axis ([10 22 93 98])
278

figure(3)
hold on
%plot(tor, kt, 'k')
288

else
figure(8);
hold on
xlabel('Torque [Nm]')
ylabel('Efficiency %')
title('Efficiency plot motor/controller/set 1100rpm')
% plot(tor,vec(:,1),'r', tor,vec(:,2), 'm', tor,vec(:,3), 'b', tor,N, 'g')
errorbar(tor, smooth(vec(:,1)), E(:,1)/2,'r')
errorbar(tor, smooth(vec(:,2)), E(:,2)/2,'k')
errorbar(tor, smooth(vec(:,3)), E(:,3)/2,'b')
legend('eff. controller','eff.motor','eff. set','motor model',4);
axis ([10 22 91 98])
293

figure(9)
hold on
xlabel('Torque [Nm]')
ylabel('Efficiency %')
title('Efficiency plot motor 1100rpm')
plot( tor,smooth(vec(:,2)), 'r', tor,N, 'g')
legend('Smoothed eff.motor','Model eff. motor',4);
axis ([10 22 93 98])
303

figure(3)
hold on
%plot(tor, kt, 'g')
308

end
313

318

pause;
clear all
clc
end
323

```

D.4 MatlabComparison between csiro motor and surface draw

```

%surface plot comparison between biel and Csiro motor
close all
clear all
clc
1

%loading date from the calculated en measured efficiency and torque
6

%loading 800 rpm data
t800_2=load('gemtorque800_2.txt');
e800_2=load('eff800_2.txt');
t800_3=load('gemtorque800_3.txt');
e800_3=load('eff800_3.txt');
11

```

```

182=length(e800_2);
183=length(e800_3);
t800=(t800_2+t800_3)/2;
e800=(e800_2+e800_3)/2;
kt800=(kt(:,1)+kt(:,2))/2
%loading 900 rpm data
t900_2=load('gemtorque900_2.txt');
e900_2=load('eff900_2.txt');
t900_3=load('gemtorque900_3.txt');
e900_3=load('eff900_3.txt');
192=length(e900_2);
193=length(e900_3);
t900=(t900_2(1:17)+t900_3(1:17))/2;
e900=(e900_2(1:17,:)+e900_3(1:17,:))/2;
kt900=(kt(:,3)+kt(:,4))/2
size(e900)
%loading 1000 rpm data
t1000_3=load('gemtorque1000_3.txt');
e1000_3=load('eff1000_3.txt');
t1000_4=load('gemtorque1000_4.txt');
e1000_4=load('eff1000_4.txt');
1103=length(e1000_3);
1104=length(e1000_4);
t1000=(t1000_4(1:17)+t1000_3(1:17))/2;
e1000=(e1000_4(1:17,:)+e1000_3(1:17,:))/2;
kt1000=(kt(:,5)+kt(:,6))/2
size(e1000)
t1000_1mm_1=load('gemtorque1000_1mm_1.txt');
e1000_1mm_1=load('eff1000_1mm_1.txt');
t1000_1mm_2=load('gemtorque1000_1mm_2.txt');
e1000_1mm_2=load('eff1000_1mm_2.txt');
t1001=(t1000_1mm_1(1:16)+t1000_1mm_2(1:16))/2;
e1001=(e1000_1mm_1(1:16,:)+e1000_1mm_2(1:16,:))/2;
11011=length(e1000_1mm_1);
11012=length(e1000_1mm_2);
%loading 1100 rpm data
v1100_2=xlsread('vec1100_2');
v1100_3=xlsread('vec1100_3');
v1100_1mm_1=xlsread('vec1100_1mm_1');
v1100_1mm_2=xlsread('vec1100_1mm_2');
1112=length(v1100_2);
1113=length(v1100_3);
11111=length(v1100_1mm_1);
11112=length(v1100_1mm_2);
v1100=(v1100_2(1:17,:)+v1100_3(1:17,:))/2;
v1101=(v1100_1mm_1(1:16,:)+v1100_1mm_2(1:16,:))/2;
kt1100=(kt(:,7)+kt(:,8))/2
length(v1100);
size(v1101)
%checking the length of the vectors
l=[ 182 183;
    192 193;
    1103 1104;
    11011 11012;
    1112 1113;
    11111 11112];
%smoothing the data to remove the edges
x=[smooth(t800)';
   smooth(t900(1:17))';
   smooth(t1000)';
   smooth(v1100(:,1))']';
x1=[smooth(t1001)';
    smooth(v1101(:,1))']';
size(x1)
size(x)
y=[smooth(e800(:,3))';
   smooth(e900(1:17,3))';
   smooth(e1000(:,3))';
   smooth(v1100(1:17,4))']';

```

D.4. MATLABCOMPARISON BETWEEN CSIRO MOTOR AND SURFACE DRAW_{xxxxvii}

```

y1=[smooth(kt800);
smooth(kt900);
smooth(kt1000);
smooth(kt1100)]';
101

y1=[smooth(e1001(:,3))';
smooth(v1101(:,4))']';
size(y1)
106

%another check for the vector length
size(e800(:,3))
size(e900(1:17,3))
size(e1000(:,3))
size(v1100(1:17,4))
111

length(x)

%defining the matrix for the surface plot of the csiro data
s_c=[800 900 1000 1100]
s_c1=[1000 1100]
z= repmat(s_c, 17, 1);
z1= repmat(s_c1, 16, 1);
size(z)
116

%defining biel data (source Georges Arkestijn)
Tbiel=[6 12 18 24 30;
6 12 18 24 30;
6 12 18 24 30;]
121

s_b=[750 1000 1250];
Sbiel= repmat(s_b,5,1);
e75=[83.56172 88.89038 90.36977 93.3117 92.92014];
e100=[82.98791 89.27637 90.99489 94.06795 93.90795];
e125=[80.89687 88.24896 89.82224 92.59246 93.08522];
126

% effbiel1= [85.51259 84.24446 83.56172 82.98791 80.89687;
% 89.34489 88.85437 88.89038 89.27637 88.24896;
% 89.73756 89.82591 90.36977 90.99489 89.82224;
% 91.352 92.81967 93.3117 94.06795 92.59246;
% 90.26509 92.6055 92.92014 93.90795 93.08522]
131

%effbiel= [smooth(e75') smooth(e100') smooth(e125')];
136

% effbiel= [83.56172 82.98791 80.89687;
% 88.89038 89.27637 88.24896;
% 90.36977 90.99489 89.82224;
% 93.3117 94.06795 92.59246;
% 92.92014 93.90795 93.08522]
141

effbiel= [e75' e100' e125'];
146

%surface PLOT
figure(1)
hold on
grid on
surf(z, x, y)
%surf(z1, x1, y1)
surf(Sbiel, Tbiel, effbiel)
colorbar
xlabel('Speed [km/h]')
ylabel('Torque [Nm]')
zlabel('Efficiency [%]')
%colormap jet
axis([800 1100 6 30 80 96])
%shading interp
title('3D Efficiency plot comparison Biel vs CSiro')
151

figure(2)
hold on
% grid on
%surf(z, x, y')
surf(z1, x1, y1)
%surf(Sbiel, Tbiel, effbiel)
colorbar
xlabel('Speed [km/h]')
ylabel('Torque [Nm]')
zlabel('Efficiency [%]')
%colormap jet
axis([80 110 10 25 80 96])
shading interp
156
161
166
171
176

```

```
%plot of 1000 rpm
Tb=[6; 12; 18; 24; 30]
eb100=e100'
figure(3)
xlabel('Torque[Nm]')
ylabel('Efficiency [%]')
plot(t1000,e1000(:,3),Tb,eb100)
axis([8 30 85 96])
title('Efficiency plot comparison Biel set vs CSiro set at 1000rpm')
```

181

186

